8-2005

Correlation of Wear and Mechanics for Subjects having a Metal-on-Polyethylene Total Hip Arthroplasty Measured in vivo

Katherine Suzanne Alford
University of Tennessee - Knoxville

To the Graduate Council:

I am submitting herewith a thesis written by Katherine Suzanne Alford entitled "Correlation of Wear and Mechanics for Subjects having a Metal-on-Polyethylene Total Hip Arthroplasty Measured in vivo." I have examined the final electronic copy of this thesis for form and content and recommend that it be accepted in partial fulfillment of the requirements for the degree of Master of Science, with a major in Engineering Science.

Richard D. Komistek, Major Professor

We have read this thesis and recommend its acceptance:

Mohamed R. Mahfouz, Jack F. Wasserman

Accepted for the Council:
Carolyn R. Hodges

Vice Provost and Dean of the Graduate School

(Original signatures are on file with official student records.)

To the Graduate Council:

I am submitting here with a thesis written by Katherine Suzanne Alford entitled "Correlation of Wear and Mechanics for Subjects having a Metal-on-Polyethylene Total Hip Arthroplasty Measured in vivo." I have examined the final electronic copy of this thesis for form and content and recommend that it be accepted in partial fulfillment of the requirements for the degree of Master of Science, with a major in Engineering Science.

Richard D. Komistek

Major Professor

We have read this thesis and
recommend its acceptance:

Mohamed R. Mahfouz

Jack F. Wasserman

Accepted for the Council:

Anne Mayhew

Vice Chancellor and Dean of
          Graduate Studies

(Original signatures are on file with official student records.)

Correlation of Wear and Mechanics for Subjects having a Metal-on-Polyethylene Total Hip Arthroplasty Measured in vivo

**A Thesis
Presented for the
Masters of Science Degree
The University of Tennessee, Knoxville**

**Katherine Suzanne Alford
August 2005**

Dedication

This thesis is dedicated to my late Gran Gran Alford and Grandmother Ritter.

Acknowledgements

Abstract

Femoral head separation from the acetabular shell has been recorded, but clinical significance of this phenomenon has not yet been established. The objective of the study was to determine if there is a correlation between femoral head separation (sliding of the femoral head away from the acetabular cup), hip joint forces, and acetabular liner wear. Twenty subjects were strategically selected to participate in this study. All subjects were asked to perform gait on a treadmill while under fluoroscopic surveillance. The number of incidences involving femoral head separation was tallied and acetabular bearing surface forces were determined for each subject. A statistical correlation was done to determine if femoral head sliding is related to the kinetics of the hip joint. Forty percent of the subjects were determined to have greater than 0.25 mm of wear. Twelve subjects demonstrated femoral head sliding leading to separation. Ten percent of the subjects tested demonstrated both wear and separation. The forces determined at the hip joint ranged from 1.75 to 1.85 times body weight. Although it was expected that subjects having more wear would have greater magnitudes of femoral head separation, the opposite was true. Kinematic data resulted in increased force magnitudes for a subject with separation then a subject with separation.

Table of Contents

List of Tables

List of Figures

Abbreviations and Acronyms

bw   body weight

THA   Total Hip Arthroplasty

mm   millimeters

s   seconds

g   gravity

Post-op   post-operative

RSA   Roentgen Stereophotogrammetric Analysis

CAD   Computer Aided Design

MOP   Metal-on-polyethylene

COP   Ceramic-on-polyethylene

MOM   Metal-on-Metal

COC   Ceramic-on-Ceramic

Chapter 1
Background

1.1 Introduction and General Information

Total hip arthroplasty (THA) is a common procedure involving replacement of the proximal femur and the acetabulum of the pelvis. Total hip replacements are most frequently performed in cases of extreme osteoarthritis where depletion of the intercellular component of the cartilage within the hip joint causes erosion and cracking of the originally smooth, cushioned surface (Figure 1) (Norkin 1983). This condition causes the subject to experience debilitating pain during ambulation. Vascular necrosis of the femoral head and hip displaysia are also common reasons for THA surgery. THA implants manufactured today have a lifetime of approximately ten years depending on subject activity and overall well being. Revision surgeries are performed most frequently in the case of osteolysis. Osteolysis is the deformation of the bone due to wear debris from the polyethylene liner. The case of wear in polyethylene will be discussed further in the sections to follow. The number of THA surgeries in the US per year is approximately 170,000 and the number of revisions is 37,000 per year (AAOS 2003).

THA implants involve two components: a metal stem (with a modular metal or ceramic head) to replace the femur, and a metal shell with a metal, ceramic, or

Figure 1: Hip with Osteoarthritis

*www.orthogastonia.com/subject_ed/html_pages/hip/hip_osteoarthritis.htm

polyethylene liner to replace the acetabulum of the pelvis. During THA surgery the proximal femur is completely removed at the base of the femoral neck.   The intramedullary canal of the femur is reamed for placement of a cobalt chromium or titanium stem. This stem provides stability throughout the continuation of the femur as well as a new femoral neck. Attached to the implanted femoral neck is a modular ball that is used as a replacement for the femoral head. The opposing side of the joint is prepared by reaming the acetabulum for fit of a metal shell into the acetabulum of the pelvis.   The metal shell encases a liner formed to accept the new femoral head replacement (Figure 2). Total hip arthroplasty allows the subject to continue normal daily living by providing a newly resurfaced hip joint at the point where defects and/or disease have afflicted the joint bearing surface.
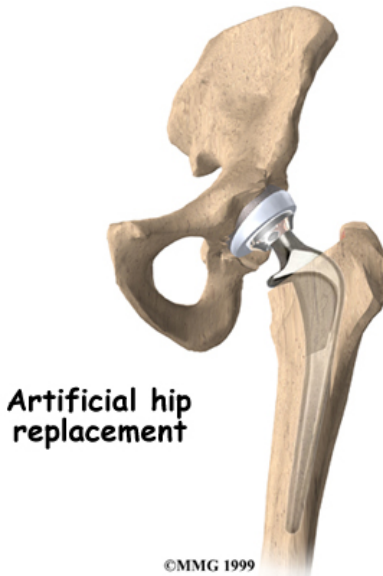
Figure 2: Total Hip Replacement*

*www.orthogastonia.com/subject_ed/html_pages/hip/hip_osteoarthritis.htm

1.2 Kinematic Predictions

THA surgical procedures are performed to return the subject to normal living standards and to provide pain relief. Research has been done on how THA affects the kinematics and kinetics of the hip joint in subjects during normal daily activities. One of the most widely studied activities is gait. Gait kinematics and kinetics have been studied using gait labs in vivo, bio-imaging techniques: Roentgen Stereophotogrammetric Analysis (RSA) and more recently, fluoroscopy.

Gait labs involve the use of multiple video cameras and light reflecting markers, placed on the subject's skin, to track the movement of the subject using a biomechanics

Figure 3: Gait Lab Markers on a Human Subject

modeling software (Figure 3). The flaw with gait lab studies is that the markers are

placed on the skin of the subject and not the actual bone or implant. Therefore, as the

subject walks, the skin stretches and the markers actually track the skin and muscle

movements instead of the bone or implants. Previous analyses have determined

significant inaccuracies with this methodology attempting to determine in vivo bone

motion (Fuller 1997, Sati 1996, Cappozzo 1991, Cheze 2000).

In vivo kinematic measurements have thus far come from two techniques: RSA

and fluoroscopy. Roentgen Stereophotogrammetric Analysis (RSA) was originally

developed by Selvik in 1974 to study micro-motion of the THA implant post-operatively.

RSA originally required the placement of tantalum beads in the THA implant and used a

computer algorithm tracking system to determine bead placement in pre-operative and post-operative images (Glyn-Jones 2004, Kaptein 2004, Selvik 1989). One of the most sought after advances in RSA has been to deride the method of the tantalum beads and use 3-D CAD models of the THA implants with the x-ray images to analyze movement (Kaptein 2004,Cianci 1995). Both approaches to the RSA method have reported high rates of accuracy; however, these methods deal with static images and therefore can not capture the true kinematics of the subject due to the lack of fluid motion between each radiograph (Ostgaard 1997, Kaptien 2004, Cinaci 1995, Sovai 1999, de Lange 1990).

The second and most recent method, fluoroscopy, allows recording of the true in vivo joint motion. Current fluoroscopy joint studies include, but are not entirely limited to, the work of researchers in our laboratory (Komistek et al, Outten 2005). Studies of the hip joint have been performed by our group for the activities of gait, abduction/adduction, and chair rise. During these studies many interesting conclusions were made. Through our previous studies of in vivo THA kinematics using fluoroscopy, the phenomena of hip separation was observed.

1.3 Separation Phenomena

Hip separation or femoral head sliding with the acetabular shell is the occurrence of the femoral head component sliding away from the center of the acetabular shell component in the superolateral direction. The design objective for THA is that the adjoining circular surfaces remain in contact and that concentric motion is evident throughout all weight-bearing activities at the hip joint. In the case of femoral head

separation, a small space is created between the two surfaces allowing the implant to slide out of its concentric boundary. Previous studies measured a leg drop motion; during this activity the subject stands on a platform and simply lets one leg dangle. This activity, one of the first tested for hip fluoroscopy, clearly detected hip separation (Figure 4).

To study the separation phenomena our lab, currently known as the Center for Musculoskeletal Research (CMR), has evaluated and compared the in vivo hip kinematics for constrained versus unconstrained THA and variable femoral head materials versus variable acetabular component materials during both abduction/adduction and gait activities (Komistek et. al). The material comparative studies have revealed that the combination of a metal femoral head component within a polyethylene liner experience the greatest amount of incidence and magnitude of femoral head separation. Komistek et al. reported that femoral head separation in MOP THA may occur because of the lack of fluid-film cohesion between the roughened polyethylene liner surface with the smooth metal femoral head surface. This rough surface area can create interferences with the adhesion of the fluid between the polyethylene liner and metal head due to interrupted contact surface area. In MOM or COC implants, the fluid-film cohesion between the smooth surfaces carries the contact of the femoral head to the acetabular shell from weight bearing stance phases of gait throughout the swing phase

Figure 4: (Top) Fully Seated Hip at Weight Bearing, (Bottom) Separated Hip at Non-Weight Bearing Dangle

(Komistek et al, Jahli-Valdid 2004, Nevelos 2000, Tipper 2002, Stewart 2003, Maso 2004). The conclusion of our group's studies has lead to the finding that hip separation most often occurs in the unconstrained MOP THA. Although many studies have documented that the phenomena of separation does occur, a further understanding of the effects of hip separation and the causes of its occurrence has not been studied or determined.

1.4 Kinetic Predictions

Due to the occurrence of THA implanted hip separation, one main question that needs evaluating is "Could femoral head separation induce impulse loading at the bearing surface caused by the impact of the femoral head into the acetabular shell under weight-bearing conditions?" There are two methods that can be used to determine in vivo force: (1) Telemetry, which is experimentally based and (2) mathematical modeling, which is theoretically based. Most previous telemetric studies involved embedded strain sensors that are placed in the implant itself to measure the bearing surface forces acting through the implant during activities. The signals are transmitted to a workstation telemetrically through a wireless device, which is also embedded inside the implant. Instrumented force measurements of the in vivo THA were first measured in 1966 by Rydell. Since then, many researchers have used telemetry in their work (Taylor 1997, Bergmann 1993, 1997, Davy 1988, English 1978). Some of the most recent work has been done by Bergmann using a COP telemetric hip to compare weight bearing surface hip forces during nine different activities: slow walking, normal walking, fast walking, walking

upstairs, walking downstairs, standing, sitting, switching weight from one to two legs, and bending the knee. Forces during normal walking were recorded in Bergmann's study in the range of 2.8 to 3.2 times body weight (Bergmann 2001). One of the most prevailing concerns with telemetry is that, over time, surface wear occurs, which often leads to the sensors becoming damaged. Long term telemetric studies of the hip joint can not be performed with today's telemetric set up. The equipment for telemetric studies is also very costly and therefore can only be used in a limited number of subjects.

The other kinetic solution is theoretical math modeling. Theoretical math modeling has been done extensively by many different methods. Most theoretical math modeling of kinematics is done using either inverse dynamics or forward dynamics. The method of inverse dynamics involves the input of kinematics to output forces and torques (math works 2005). Inverse dynamic modeling of the THA implanted hip joint has been done using the kinematic data collected from gait labs and fluoroscopy. Hip joint forces during gait kinematics gathered from lab data have been found to have a very high value and extensive range of 4-12 times body weight (Stansfield 2002, Stansfield 1998). Gait forces found using data from in vivo fluoroscopy have been found to be approximately 1.9-2.6 times body weight which is much closer to the reported telemetric data than the gait lab analysis (Komistek 1998). Forward dynamics is done using a prediction of the forces and torques to output the motions. The biggest problem with using forward dynamics however is that the models tend to be very complicated and very time

consuming to develop due to the collection of force profiles for the variables used in the study (Hof 2004).

1.5 Wear Predictions

A second question of concern pertaining to the occurrence of hip separation in a THA is whether these "non-normal" kinematic patterns may influence polyethylene wear due to decrease in contact area during femoral head separation from the acetabular shell. The wear of the polyethylene liner itself can be caused by many different effects including but not limited to improper cross-linking techniques of the polymer, sterilization techniques, abnormal kinematics, or simply by normal wear and tear of the THA implant over many years (Claus 2003, Goldsmith 2001, Masaoka 2003, McKellop 1995, Devane 1997, Komistek 1998, McKellop 1985, Northcut 1999, Ramamurti 1996). During THA many of the stabilizing muscles and ligaments are removed from the hip joint including the fibourous capsule, acetabular labrum, and the ligament at the head of the femur, the iliofemoral, ischiofemoral, pubofemoral, and transverse acetabular ligaments (Clarke 2003, Crowninsheield 1978). Absence of these ligament-force interactions may also play a role in abnormal femoral head/acetabular shell movement and polyethylene wear.

Tracking of femoral head movement on the acetabular shell to predict wear patterns has been done with hip joint simulators (Clarke 1997, Ramamurti 1996, Saikko 1993, Clarke 1997, McKellp 1984). Hip simulations have been conducted using experimental wear simulators for COC THA under femoral head separation conditions,

revealing for the first time similar wear patterns and modes of wear when comparing retrieval specimens with simulation specimens (Masao 2004, Tipper 2002). Only one study has simulated MOP THA and found that implant wear and separation are negatively correlated (Clarke 2005).

The current acetabular liners manufactured are composed of ultra high molecular weight polyethylene (UHMWPE), which is a highly crosslinked polyethylene material processed by radiation. During the processing, radiation is used to reduce the numbers of free radicals in the material that may cause oxidation. By eliminating the free radicals, the chains of the polyethylene tend to crosslink properly. Although this new crosslinked polyethylene is much more wear resistant, wear does remain a concern and long-term follow-up has not been established for this material. One major concern for wear is that the debris particles caused by wear of the polyethylene liner can cause osteolysis. Osteolysis causes bone softening and degradation, eventually requiring revision surgery to pack deformations in the bone and replace the implant. During osteolysis the macrophages of the body engulf the polyethylene debris particles. Unable to process the foreign material, the macrophages release a toxic substance that in turn degrades the bone. Wear can occur between the implant and bone interfaces as well as between the implant components themselves. The current study focuses on the wear between the femoral head and the acetabular liner.

The purpose of the current project is to determine if the abnormal impulse loading of the THA implant caused by hip separation is evident in subjects having a MOP THA

with and without wear of the polyethylene. Our hypothesis is that during gait and other weight-bearing activities, femoral head separation may induce greater shear stresses at the bearing surface of the THA, possibly leading to increased polyethylene wear. Due to the influence of hip separation it is also assumed that subjects having a higher incidence and magnitude of femoral head separation may have greater wear of their polyethylene insert. It was also assumed that subjects with femoral head separation may also have increased bearing surface forces at the THA interface. Therefore it is thought and hypothesized that abnormal hip kinematics (differing from the normal hip) may cause impulse loading conditions to be prevalent and that the cyclic impulse motions of the femoral head sliding on the superolateral aspect of the acetabular shell induce shear stresses between the two components and subsequently cause more wear to occur.

Chapter 2

Material and Methods

2.1 Subject Selection

A total of twenty volunteer subjects were enrolled in the study. The request for subject participation was accepted through the IRB # 897-A and all subjects were informed of the procedures. Each person was then asked to sign a statement of participation as well as a Health Insurance Portability and Accountability Act (HIPPA) privacy form. In addition, subjects were asked to fill out a survey describing their own opinions on their post-operative experience and overall satisfaction with their current quality of life (Appendix).

All subjects had a total hip arthroplasty and were subjects from a single surgeon (Dr. Douglas A. Dennis, Colorado Joint Replacement, Denver, Colorado). A single surgeon was used as a control for surgical technique and THA implant functionality in the study, which we hoped would help control the number of variables. Traditionally, there are two basic types of hip arthroplasty surgical techniques; (1) the posterolateral approach, and (2) the anterolateral approach. It has been suggested that the posterolateral approach has a higher correlation with dislocation problems than the anterolateral

approach, due to the cut of the posterior capsule and short external rotators that stabilizes the joint (Madsen 2004, Schinsky 2003, Weeden 2003). No specific studies have been done to determine the effects of differing surgical approaches on separation; therefore to reduce surgical variance, subject selection was limited to the one surgeon using the same surgical approach on each subject. Therefore, all subjects in this study were implanted using posterolateral approach.

The subjects selected in this study all have similar MOP THA implants manufactured by the same company (DePuy, A company of Johnson and Johnson Company). All subjects were at least three years post-operative. Stems used for this study included a variation of sizes from DePuy's Ultima series, Unirom series, Stability series, S-rom series, and PFC series. Stem geometry can play a role in implant wear; however in this study geometry was not included for the simple reasoning of limited subject resources and research time. Femoral head sizes were mainly 28 mm in diameter with the exception of one subject having a 26 mm femoral head. The offsets of the femoral heads ranged from 0-12 mm. Researchers have studied the effect of variation of femoral head size in relation to wear of the liner. One such study concluded that femoral head size does influence wear. (Murtalog 2001) Normal polyethylene wear time can vary for different UHMWPE processing techniques. It has been reported that the wear rate for marathon liners is approximately 0.08-0.24 mm/year while Enduron liners is 0.18-0.2 mm/year. Both liner types had been sterilized with gas plasma; however the Marathon liners were irradiated at five Mrad to diminish all free radicals and the Enduron liners

were not (Hopper 2003). The polyethylene liners in the current study included Marathon, Enduron, Hylamer, and PFC. An overall typical estimated average of wear in MOP THA implants is approximately 0.05-0.1 mm/year depending on subject activity and polyethylene processing quality (Walker 2002).

In order to ensure quality performance of the requested gait activity, all subjects were required to be active and have a Harris Hip Score (HHS) greater than 90. The Harris Hip Score is a rating of how active the subject is with their daily activities, such as tying a shoe, bending down, sitting in a chair, etc (Stryker 2005). A score of greater than 90 corresponds to a subject who is able to do 90% of their daily activities with little to no difficulty. The subjects in this study consisted of eleven males and nine females having an average age of 64 years (range of 44-79). The following methods were used to analyze the twenty subjects for wear, separation, and gait kinematics.

2.2 Fluoroscopy

All subjects performed treadmill gait while under fluoroscopic surveillance using a VF-2000 fluoroscope (Radiographic and Data Solutions, Inc., Minneapolis, MN) operated by a certified radiation technician, allowing for the documentation of the relative motion between the femoral and acetabular components under in vivo conditions. The use of fluoroscopy allows for the formation of a basic projection image, captured by passing pulsated radiation through the subject's joint and onto an image intensifier (usually a ten to twelve inch diameter circle). The amount of radiation emitted from
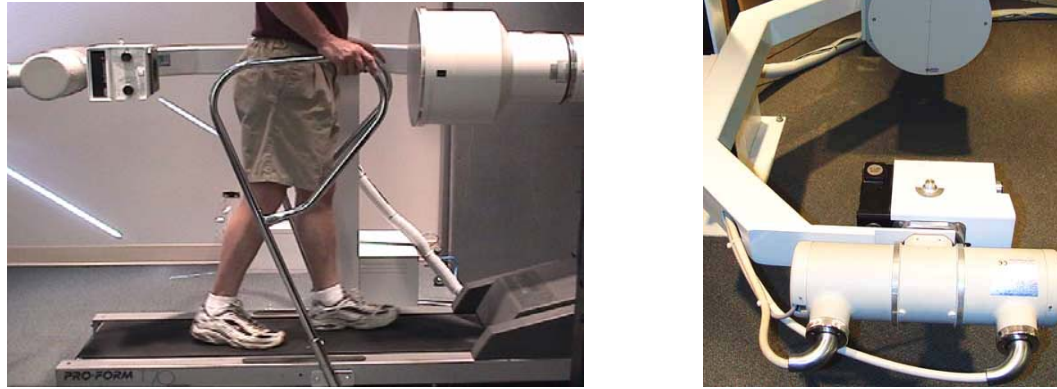
Figure 5: (Left) Fluoroscopy Machine with Treadmill and Subject (Right) Top View of Fluoroscopy Machine, Image of Radiation Source to Image Intensifier

pulsated fluoroscopy, measured at the maximum setting was 2.4 rad/min (3.6 Rem), which is much less than steady stream x-ray having a continuous stream of radiation. The image intensifier passed the image onto a mirrored system into a camera which recorded the dynamic movements (Figure 5).

The metal femoral stem and acetabular shell containing the polyethylene liner appeared as a blackened silhouette on the video screen (Figure 6). Bone and tissue were viewed surrounding the THA implant as lighter gray areas due to better passivity of the radiation. The fluoroscopic video was captured at 30 frames per-second in order to gain the best quality images. The speed of the treadmill was monitored such that it was at a rate that would allow the images to be captured without occurrence of blurring or ghosting. The fluoroscopic video was recorded onto a digital video (DV) recording

Figure 6: Picture on Picture View of Fluoroscopy Image with Real Time Image

system. The real-time video of the subject's stride was also captured using a video home system (VHS) camcorder. Both the fluoroscopic video and real-time video were collaborated onto one screen using a picture-on-picture box (Figure 6). This created a screen view of the subjects gait cycle in vivo and ex-vivo, allowing use of a visual aid in determining what instance of the gait cycle was being captured. Specified frames from the fluoroscopic gait videos for each subject were captured and edited using the software package Adobe Premiere Pro[TM]. Images were taken at heel-strike, 33% of stance phase, 66% of stance phase, toe-off, and at six increments of swing phase for each subject. Gait phases were determined using the picture-on-picture image of the real-time subject gait cycle. For example, when the real-time video of the activity showed the subject in heel-strike, the adjoining fluoro-video frame was captured. Values of 33% and 66% of stance

phase were found by calculating the number of frames between heel-strike and toe-off. This value was then divided by three and added in succession from the first heel-strike value. Swing phases were found by using the time between the toe-off and the next heel-strike in gait. This time was divided by six and added in succession from toe-off to find all six swing phases. The settings for capturing images from the DV video were 640 X 480 frame size at 0.1 pixel ratio, and images were saved in tiff format to ensure the best possible resolution properties.

Images captured from the fluoroscopy were initially geometrically distorted by an effect called pin cushioning, created by the distance between the x-ray source and the image intensifier. This effect caused the pixels of the images to concave inwards leading to the images to appear to be warped. To unwarp the images, a calibration method was performed using a fluoroscopic image of a bead board. The bead board consisted of a clear plexi-glass plate with metal beads inserted at a known distance apart from each other in grid format (Figure 7). The letter "B" was also placed on the board to observe whether the fluoroscopy unit inverted the images. The bead board fluoroscopic image was used to estimate the geometrical distortion by an algorithm in Matlab^{TM}. The Matlab code estimated each 2-D spatial transform of the four bead bounded blocks throughout the board and applied a local bilinear mapping model and gray level interpolation method to remove the distortion (Mahfouz 2003). Overall the Matlab process found the digital pixel locations of the beads in the board (state space), compared
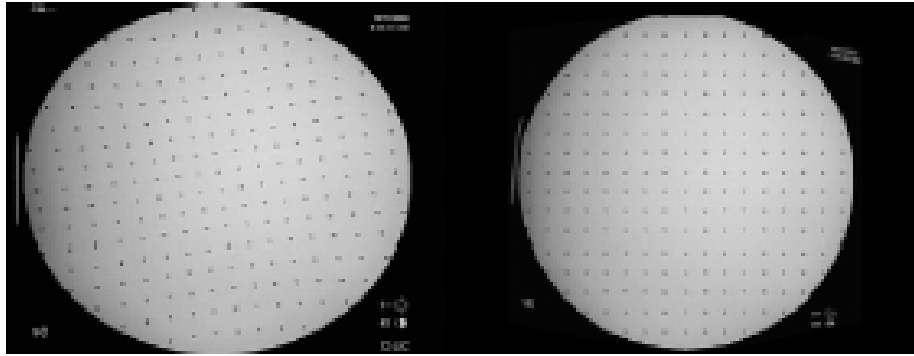
**Figure 7: (Left) Original Fluoroscopy Image of a Warped Calibration Bead Board
(Right) Un-warped Fluoroscopy Image of the Calibration Bead Board**

it with the known bead distances, and then created a transform function to calibrate all of

the fluoroscopy images from state space back to the true bead board geometries. This

process was used to unwarp all images taken by the particular fluoroscopy machine.

2.3 2-D to 3-D Registration Analysis

Using CAD drawing software, 3-D models of the femoral stem and acetabular

shell THA implants were drawn based on model drafts provided by the company. The

CAD models and 2-D gait images were then analyzed for wear and kinematics using a 2-

D to 3-D registration method. Metal implants were viewed as darkened silhouettes in the

fluoroscopic images because of the lack of radiation transmission through the metallic

materials. Polyethylene absorbs radiation and was transparent in the fluoroscopic

images; therefore, the metal shell encasing the polyethylene liner was used for

referencing. The darkened implant silhouettes on the 2-D fluoroscopic images were used
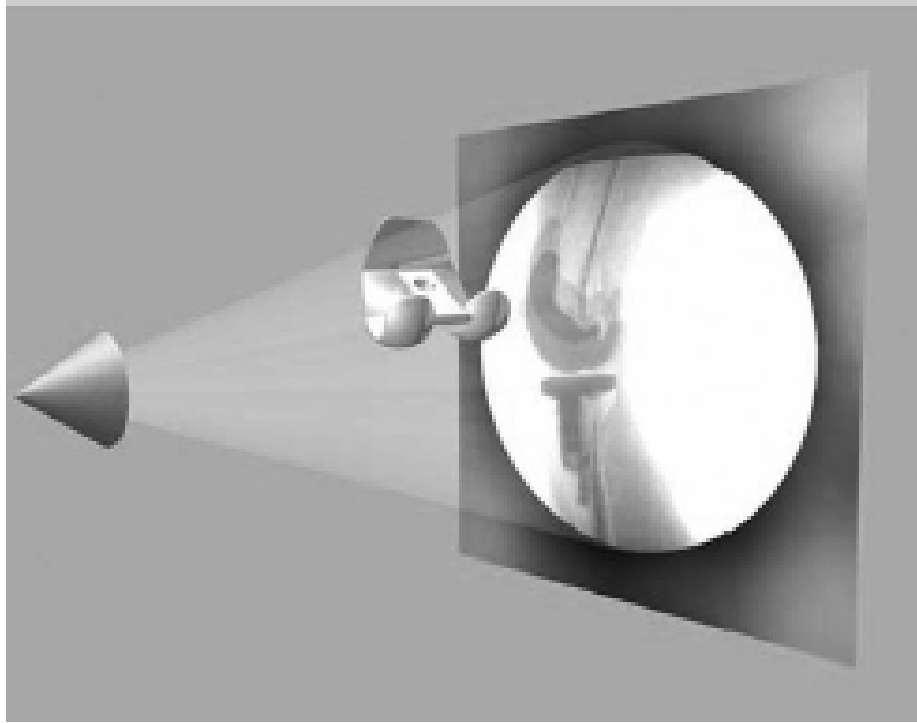
Figure 8: 3-D CAD Model Matching Projected Fluoroscopy Image Silhouette

as a base location for predicting the location of the 3-D implant models in-vivo (Figure

8). The registration method used for this study contained a combination of a matching

algorithm, optimization technique, and supervisory control to create the analysis

(Mahfouz 2003). The matching algorithm compared a predicted image formed from the

3-D CAD drawing using SGI^{TM} and Open Inventor^{TM} to the actual fluoroscopic image.

The two images are evaluated by a combination of their pixel values (intensity matching

score) and edge detection (contour matching score) determined by:

Intensity Matching Score: $= \dfrac{\sum\limits_{(x,y)} G(x,y)H(x,y)}{\sum\limits_{(x,y)} H(x,y)}$,

where   G(x, y) = input x-ray image

H(x, y) = predicted x-ray image

Contour Matching Score: $= \dfrac{\sum\limits_{(x,y)} J(x,y)K(x,y) / \sum\limits_{(x,y)} K(x,y)}{}$,

where   J(x, y) = the input edge-enhanced image

K(x, y) = the predicted edge image

Both scores are highest when their pixel values or counter values match the silhouette with the CAD model. Combining the scores and finding the minimum value allows the algorithm to know what location is the best possible match. With semi-symmetrical implants such as knees, the combination of scores can create two local minimums. Out of the two scores only one can be possible and therefore the true minimum value must be found. To do this, an optimization algorithm is run using seven possible location points starting from the worst possible case and iterating until the best scenario is found. The final step is the supervisory controls which allow the user to define their ideal input on where the model should be located. During THA analysis the supervisory controls are used a majority of the time. Unfortunately, due to the density of the muscle and fat tissue around the hip joint, running the matching and optimization techniques did not always work. The cylindrical symmetry of the acetabular shell models also caused a problem with the algorithm causing it to run continuously and never find the perfect match to the silhouette. The stem and acetabular shell models were most often manually fit by the user alone.

Threshold analysis of the 2-D to 3-D registration system has shown translational error to be approximately 0.1 mm (with exception of the Z-direction) and rotational error to be 0.4 degrees under ideal conditions. Experiments have been performed by Mahfouz et al. to determine this threshold by comparison of values taken from three different setups. One setup included manually placing the implants in known positions in front of the fluoroscopy machine, taking the image, overlaying the image, and comparing the numbers. Another setup involved implanted cadaver legs which were monitored by an Optotrack system as well as the fluoroscopy machine. The final test used real human subjects. Studies using Mahfouz's 2-D to 3-D registration analysis thus far have used a threshold of 0.75 mm for error elimination purposes. A threshold analysis was done for the images used in the current study by a simple linear measurement calibration done using Sigma Scan^{TM}. Captured fluoroscopic images were imported into Sigma Scan which allowed linear measurements to be taken of the diameter of the femoral head in pixel values (Figure 9). The known diameter of the femoral head was then used along with the pixel measurements to find the millimeter/pixel values of the images. Dynamic images were found to have a value of 0.55 mm/pixel and were therefore chosen as the threshold for the gait cycle captured images. Since movement of the subject can cause slight blurring of the contours, it was decided that the threshold for the wear analysis could be as small as 0.25 mm. This kept the dynamic images within one standard
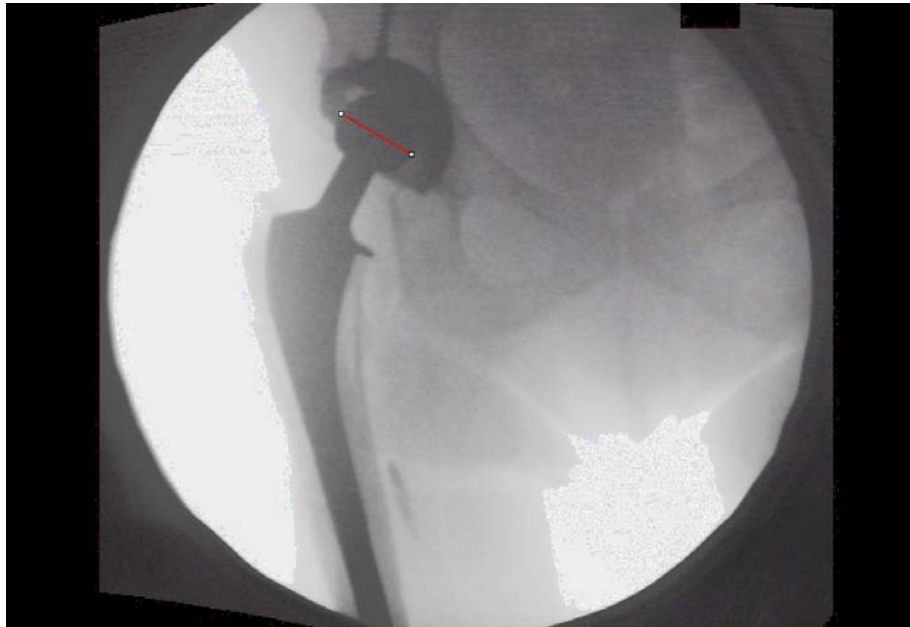
Figure 9: Sigma Scan Measurement of Femoral Head Diameter

deviation away from the standstill images and still well above the predicted threshold of

the system at 0.1 mm for a safety factor.

2.3.1   Wear Analysis

Weight-bearing stationary images were evaluated using the above 2-D to 3-D

registration algorithm to determine a predicted measure of polyethylene wear of the shell

liner. Each acetabular shell component consisted of a polyethylene liner with a metal

shell backing. As mentioned earlier, since the polyethylene component was not visible in

the fluoroscopic images, the metal acetabular shell was used as a measuring reference.

The liner measured thickness between the metal femoral head to the metal acetabular

shell was first obtained (Figure 10). The measured thickness was then subtracted from
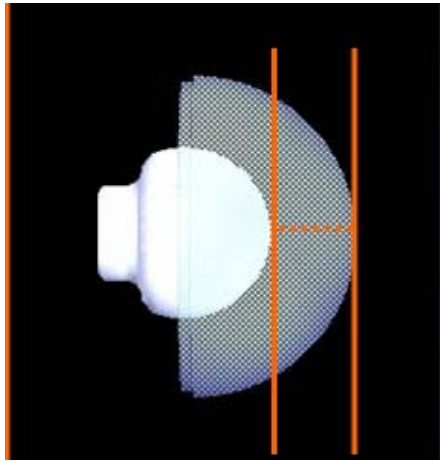
Figure 10: Wear Measurement from Proximal Femoral Head to 0uter Proximal Edge of Acetabular Shell

the known thickness of the implanted polyethylene liner and metal shell combined, to determine the amount polyethylene wear. A threshold of 0.25 mm was used for the current analysis of wear. This meant that any values greater than or equal to 0.25 mm were determined as having wear in this study.

2.3.2 Separation Analysis

Separation analysis was performed in a similar procedure to wear analysis. The registration algorithm allowed the user to overlay the 3-D models onto the 2-D fluoroscopic gait cycle images captured from the fluoroscopic videos (Figure 11). The overlay method created an image analysis of the implants over the entire dynamic gait cycle. Using the 2-D to 3-D registration algorithm, linear separation measurements were calculated from the most proximal point of the femoral head to the proximal acetabular
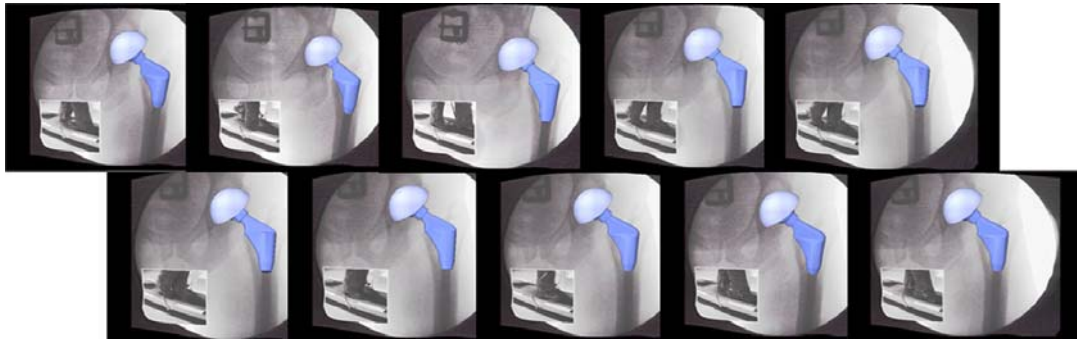
Figure 11: Full Sequence of Analyzed Images in the 2-D to 3-D Registration System with 3-D Models Overlaid

shell edge during each frame captured (Figure 12).The 2-D to 3-D registration software also recorded the models positions throughout the gait cycle. All models were centered before input at the origin (0, 0, 0) in the program reference frame. As the models were manipulated individually, the rotations and translations from the original position were recorded for the program's set X, Y, and Z reference frame (Figure 13). The kinematic equations were used in the mathematical model described later. A threshold was chosen for the dynamic analysis at one standard deviation away from the wear analysis to compensate for possible blurring of the implant silhouettes created during the gait motion, at 0.55 mm.

2.4 Theoretical Modeling

A basic 3-D mathematical model using Kane's method of dynamics was created to model hip joint mechanics in vivo. A 3-D model for the current study includes only
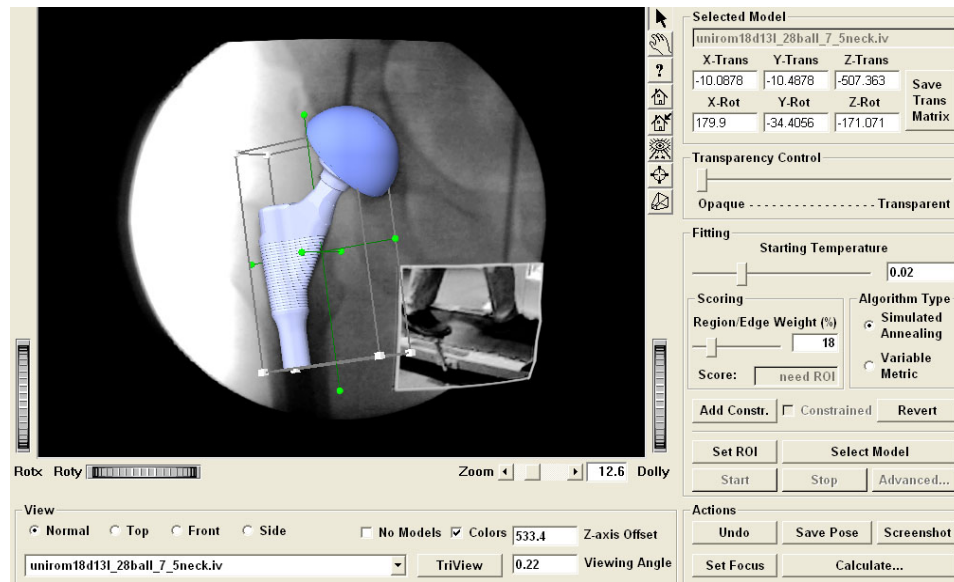
Figure 12: Separation Measurement Analysis from Proximal End of Femoral Head to Proximal End of the Acetabular Shell
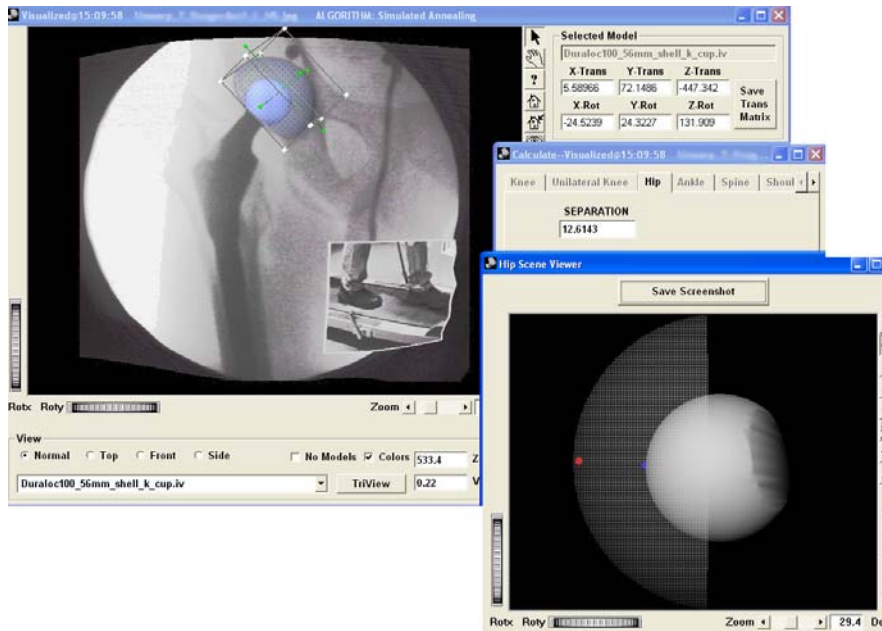
Figure 13: Translation and Rotation Recordings in the 2-D to 3-D Registration Algorithm

two rigid bodies: the femur (Body A) and the pelvis (Body B) with six degrees of freedom three for each body. A Newtonian reference frame, N, was set, as well as sequential massless (intermediate) frames for each body, A and B (Figure 14).

2.4.1 Modeling Assumptions

The following assumptions were made for this model. Muscles and ligaments were not included in the model for simplification reasons and were viewed as being inclusive factors of the forces and torques solved for between the femur and acetabulum. The motion of the femur with the respect to the pelvis was viewed in three rotations: flexion/extension, internal/external, and abduction/adduction. The motion of the pelvis with respect to the femur was only replicated in flexion and extension due to the lack of
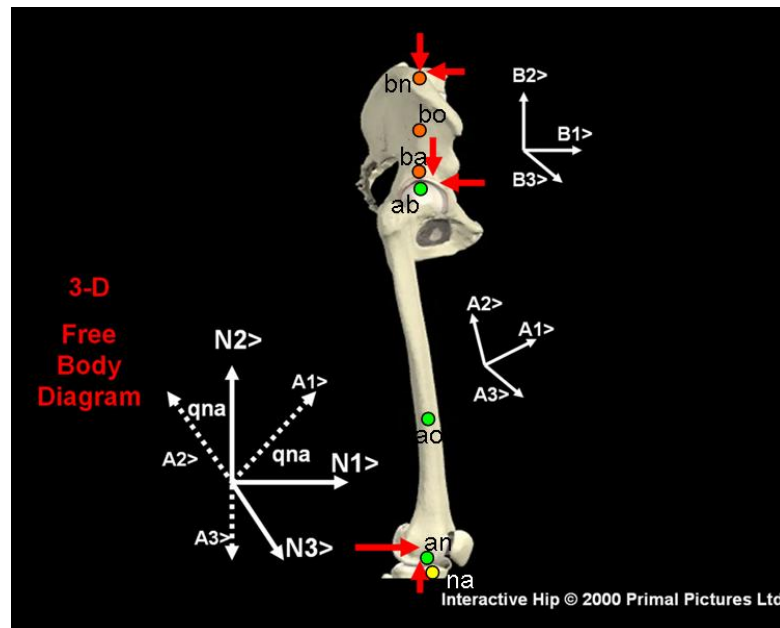
Figure 14: 3-D Free Body Diagram of the Hip Joint for Theoretical Modeling
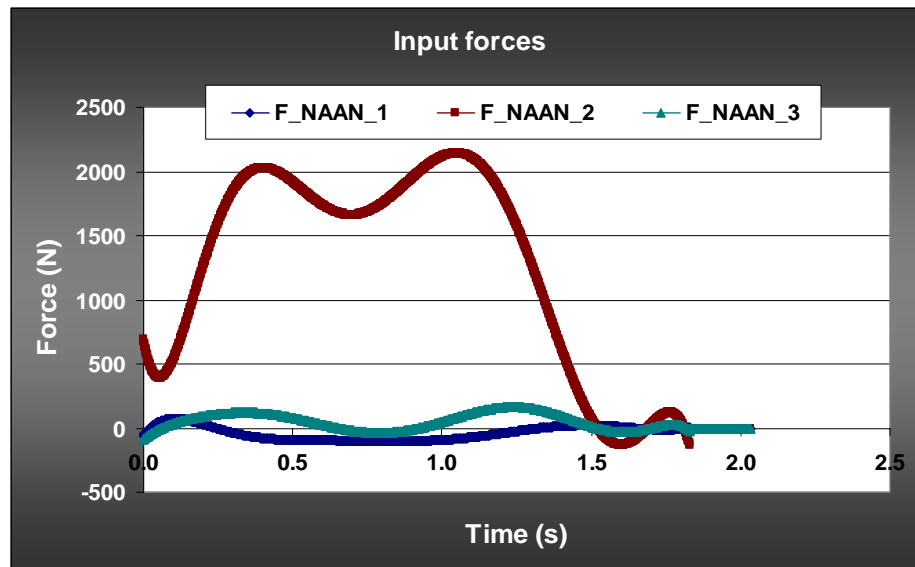
Figure 15: Force Plate Data Gathered and Doubled for Code Input

movement of the pelvis in abduction/adduction and internal/external rotation during gait.

Only principle moments of inertia were included for each of the rigid bodies. All other

inertia values were assumed insignificant due to the complexity of the system. Forces

were input into the model at the distal end of the femur from force plate data collected

from a gait activity of one subject in this study. During the activity, a volunteer walked

across the force plate in normal stride making sure to get the entire stance phase of gait

from one foot on the force plate (Figure 15).   Using the results from our previous

mathematical models of the knee joint and the results from a telemetric knee we decided

to input a temporal forcing function at the femorotibial articulation having a maximum

force of 2.0 times body weight (D'Lima 2005, Komistek 1998). Therefore, the function

at the femorotibial joint represented a forcing function that was 2.0 times the forcing

function derived between the foot and the force-plate.   Using this assumption, we normalized the force-plate data for each subject using their body-weight and their stride distance. No other forces were used as inputs and the hip joint was assumed frictionless.

2.4.2   Kane and Levinson's Method

As stated previously, we chose Kane's method of dynamics to formulate the system equations of motion. Based off of Newton's theory, the basic equation for Kane's method is:

$$F_r + F_r^* = 0 \quad r = 1,.....,n$$

The above equation defines the sum of generalized active (F_r) and inertial forces for each generalized speed equal to zero (F_r^*):

"Kane's equation" may look more familiar in the form:

$$F - ma = 0$$

This is an alteration of Newton's law of motion:

$$F = kma = k \bullet (mv)$$

where mv = linear momentum,

F = applied force, and k = a unit dependent constant

Generalized active forces (F_r) are a combination of the constrained and unconstrained generalized active forces in the dynamic problem defined with partial velocities and partial angular accelerations.

$$F_r = \sum_{u=1}^{N} [\ {}^A\underline{V}^S_{Ur} \bullet \underline{F}^S + {}^A\underline{\omega}^S_{Ur} \bullet \underline{T}^S\ ],$$

Generalized inertial forces (F_r^*) are a combination of the constrained and unconstrained generalized inertial forces of the dynamic problem.

$$F_r^* = \sum_{u=1}^{N} [{}^A\underline{V}^S_{Ur} \bullet \underline{F}^{S*} + {}^A\omega^S_{Ur} \bullet T^{S*}]$$

where

r = the rth degree of freedom

n = the total number of degrees of freedom (in this case 3 per body)

N = the number of rigid bodies in the system (in this case 2)

U_r = the rth generalized coordinate

S = the body being referenced

A = the coordinate of the fixed reference frame

${}^A\underline{V}^S_{Ur}$ = the partial velocity or partial derivative of the of change in distance between the position and mass center velocity vector in the rigid body in question

${}^A\underline{\omega}^S_{Ur}$ = the partial angular acceleration or the derivative of the orientation of the angular velocity vector on the rigid body in question

F^S = the resultant force acting on the body in question

T^S = the resultant torque acting on the body in question

F^{S*} = the resultant inertia force on the body in question

T^{S*} = the resultant inertia torque on the body in question

Partial velocities and partial angular accelerations were expressed as:

$$^{A}\underline{V}^{S}{}_{Ur} = \frac{\partial^{A}\underline{V}^{S}}{\partial U_{r}} ,$$

where, $^{A}\underline{V}^{S}$ = the velocity vector of the mass center of rigid body S

relative to the origin of the fixed referenced axes

$$^{A}\underline{\omega}^{S}{}_{Ur} = \frac{\partial^{A}\underline{\omega}^{S}}{\partial U_{r}}$$

where, $^{A}\underline{\omega}^{S}$ = the angular velocity vector of the rigid body S

The resultant inertia force ($\underline{F}^{S*}$) and torques ($\underline{T}^{S*}$) are defined by:

$$\underline{F}^{S} = -M^{S} \bullet \underline{A}^{S} ,$$

$$\underline{T}^{S*} = -(\underline{\underline{I}}^{S} \bullet {}^{A}\underline{\omega}^{S}) \times {}^{A}\underline{\omega}^{S} - \underline{\underline{I}}^{S} \bullet {}^{A}\underline{\alpha}^{S} ,$$

where, M_{s} = the mass of rigid body S

$\underline{A}^{s}$ = the acceleration vector of the mass center of the Sth rigid body

relative to the origin of the fixed referenced axis

$^{A}\underline{\alpha}^{S}$ = the angular acceleration vector of the Sth rigid body

$\underline{\underline{I}}^{S}$ = the inertia dyadic of the Sth rigid body [Komistek 1992]

Six degrees of freedom were defined for each body, creating twelve total degrees of freedom in the system, and twelve generalized speeds were created and constrained. As mentioned earlier intermediate frames, or better known as generalized coordinates were defined for each body. Generalized coordinates ($q_{r}, r = ,...,n$) act as time varying rotations and translations defining all point and rigid body orientations. Generalized

speeds (U_r) then can be set to simplify calculations the time varying functions of the generalized coordinates.

$$U_r \quad = \quad \sum_{s=1}^{r}[Y_{rs}q_s + Z_r]$$

where, 'Y_{rs}' *and* 'Z_r' are functions of the generalized coordinates and time (Sharma 2005).

Generalized speeds were introduced into the angular acceleration and six into the velocity equations.

$$^A\underline{\omega}^N \quad = U_1\,\underline{I}_u + U_2\underline{K}_u + U_3\underline{J}_u \ ,$$

$$^B\underline{\omega}^A \quad = U_4\,\underline{I}_u + U_5\,\underline{K}_u + U_6\underline{J}_u \ ,$$

$$^B\underline{\omega}^N \quad = U_1\,\underline{I}_u + U_2\underline{K}_u + U_3\underline{J}_u + U_4\,\underline{I}_u + U_5\,\underline{K}_u + U_6\underline{J}_u$$

where, $\quad$ *A* $\quad$ = the generalized coordinate of the rigid body of the femur

$\quad$ *B* $\quad$ = the generalized coordinate of the rigid body of the pelvis

$\quad$ *N* $\quad$ = the Newtonian or fixed reference frame

The remaining six generalized speeds were placed into the velocity equations in a similar fashion using points defined on the rigid bodies. Velocities were defined from the distal end of each rigid body.

2.4.3 Dynamics

Equations of motion were formed from rotational and translational data of the femur with respect to the pelvis, collected from the kinematics found in the fluoroscopic analysis. As mentioned in the assumption, rotations were modeled to describe the

movement of the pelvis with respect to the femur. Rotational sequences were described

in the order of greatest amount of rotation to the least amount of rotation:

The direction of cosine matrices created for the leg kinematics are:

For the femur:

1.   Flexion/Extension

$$= \begin{pmatrix} \cos(q3) & -\sin(q3) & 0 \\ \sin(q3) & \cos(q3) & 0 \\ 0 & 0 & 1 \end{pmatrix}$$

2.   Abduction/Adduction

$$= \begin{pmatrix} 1 & 0 & 0 \\ 0 & \cos(q1) & -\sin(q1) \\ 0 & \sin(q1) & \cos(q1) \end{pmatrix}$$

3.   Internal/External

$$= \begin{pmatrix} \cos(q2) & 0 & \sin(q2) \\ 0 & 1 & 0 \\ -\sin(q2) & 0 & \cos(q2) \end{pmatrix}$$

From the individual frame rotations the full transformation of body A with respect to the

Newtonian reference frame was determined.

For the pelvis

1.   Flexion/Extension

$$= \begin{pmatrix} \cos(-q3) & -\sin(-q3) & 0 \\ \sin(-q3) & \cos(-q3) & 0 \\ 0 & 0 & 1 \end{pmatrix}$$

The current model has some unique features. First, the input data in this model is derived using in vivo methodologies that allows for subject specific data to be used. Secondly, the model is parametric in natured allowing for unique conditions to be modeled for each subject, including the occurrence of femoral head separation (femoral head sliding in the acetabular cup) from the acetabular liner Finally, this model was derived as a system of equations, rather than using traditional mechanics approaches that models each rigid body separately. Translation vectors between defined points on respective rigid bodies (example: from the center of the femur to the center of the pelvis, point ao to point bo on the free body diagram) where were derived under in vivo conditions and then temporal functions were derived by curve-fitting the data points with respect to time. Constant vectors of lengths were defined for the femur and the pelvis. Lengths of the bodies were defined:

$$\underline{PF} = PF_1\underline{I} + PF_2\underline{J} + PF_3\underline{K} \quad \text{(distal femur to femur center of mass)}$$

$$\underline{PD} = PD_1\underline{I} + PD_2\underline{J} + PD_3\underline{K} \quad \text{(distal femur to proximal femur)}$$

$$\underline{PP} = PP_1\underline{I} + PP_2\underline{J} + PP_3\underline{K} \quad \text{(distal pelvis to pelvic center of mass)}$$

$$\underline{PE} = PE_1\underline{I} + PE_2\underline{J} + PE_3\underline{K} \quad \text{(distal pelvis to pelvic-lumbar boundary)}$$

Position vectors for the pelvis were completed in the same fashion as those for the femur but with respect to the defined "B" reference frame. The bodies were now

Table 1: Measurements Used for Anthropometry Data

GENDER	PELVIS	CENTER OF MASS	THIGH	CENTER OF MASS
Male	251.7 mm	106 mm	520.2 mm	236.6 mm
Female	256.8 mm	128.4 mm	496.2 mm	248.1 mm

registered in the Newtonian reference frame in their respective orientations. A note must be made that anthropometric data was not taken at the time of fluoroscopy. Estimation of subject lower limb data for an average male and average female was used from Leva's paper (Leva 1995). The values used for the specific anthropometric inputs of this study are above in Table 1.

Using the position vectors, velocities, and angular velocities described above along with twelve equations of motion input from the kinematic data, generalized forces and generalized inertias were derived. In a solvable system the number of unknowns equals the number of knowns.

Since twelve equations of motions were placed into the mathematical model, twelve outputs could be derived. The outputs chosen for this model were:

FHIPI>,FHIPJ>,FHIPK>   = forces between the proximal femur and acetabulum of the pelvis

THIPI>,THIPJ>,THIPK>	= Torque between the proximal femur and acetabulum of the pelvis
FPLI>,FPLJ>,FPLK>	= Force between the pelvis and lower lumbar
TPLI>,TPLJ>,TPLK>	= Torque at between the pelvis and lower lumbar

Resultant forces and torques could also be solved for with simple addition:

$$FHIP> = FHIPI> + FHIPJ> + FHIPK> ,$$

$$THIP> = THIPI> + THIPJ> + THIPK> ,$$

$$FPL> = FPLI> + FPLJ> + FPLK> ,$$

$$TPL> = TPLI> + TPLJ> + TPLK>$$

Chapter 3

Results

3.1 2-D to 3-D Registration Analysis

Forty percent of the subjects had wear rates above the threshold value of 0.25 mm. Wear was determined overall insignificant in the group. Wear values ranged from 0 to 2.9 mm and all data gathered was initially compared with post-operative times to determine if there was a correlation (Figure 16). The appearance of negative wear rates in some subjects (forty-percent of the subjects) was actually the occurrence of , femoral head separation, which will be discussed in a later section. Also, there was not a statistical correlation between wear and post-operative time. The insignificance of post-operative time to wear was a surprise, however it could be due to the fact that forty-percent of the subjects had negative wear values, which made wear in those subjects indistinguishable from separation.

Another surprising finding was that the subject experiencing the maximum amount of wear was just over three year's post-operative. A graph of the subjects wear values along with separation values throughout the gait cycle is also shown below (Figure 17). A comparison of one of the subjects with no wear or separation is also provided
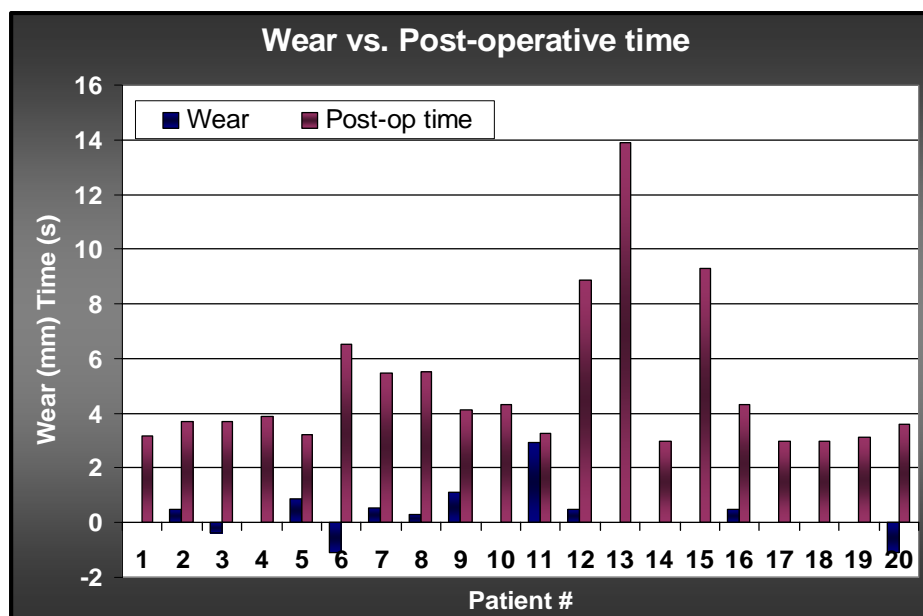
Figure 16: Wear vs. Post-operative Analysis for All Twenty Subjects

(Figure 17). In further analysis of the subject surveys it was noted that this particular subject had confessed to being a champion tennis player at his local country club before his total hip arthroplasty and was unable to give up the habit. The surgeon was advised of the subjects high wear values and agreed to monitor the subject's THA implant more closely at the follow-up visits. As mentioned earlier, "negative" wear values were found in twenty-five percent of the subjects. These subjects were also determined to have separation values, thus leading to the conclusion that femoral edge loading must be occurring. Femoral edge loading occurred when the subject's wear was centralized on the edge of the acetabular shell. The edge wear allowed the femoral head to slide to the lateral edge of the shell at all times, even during weight bearing stand still (Figure 18).
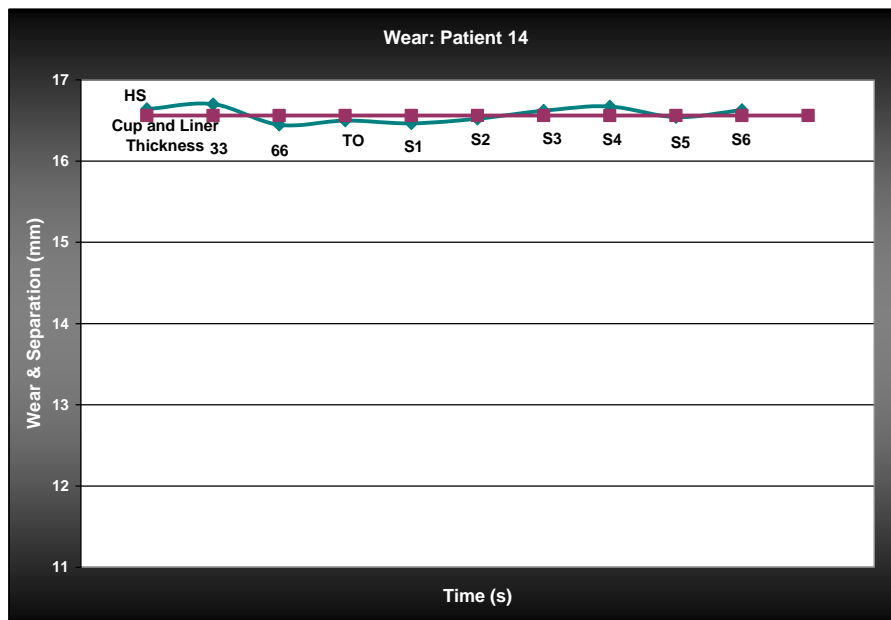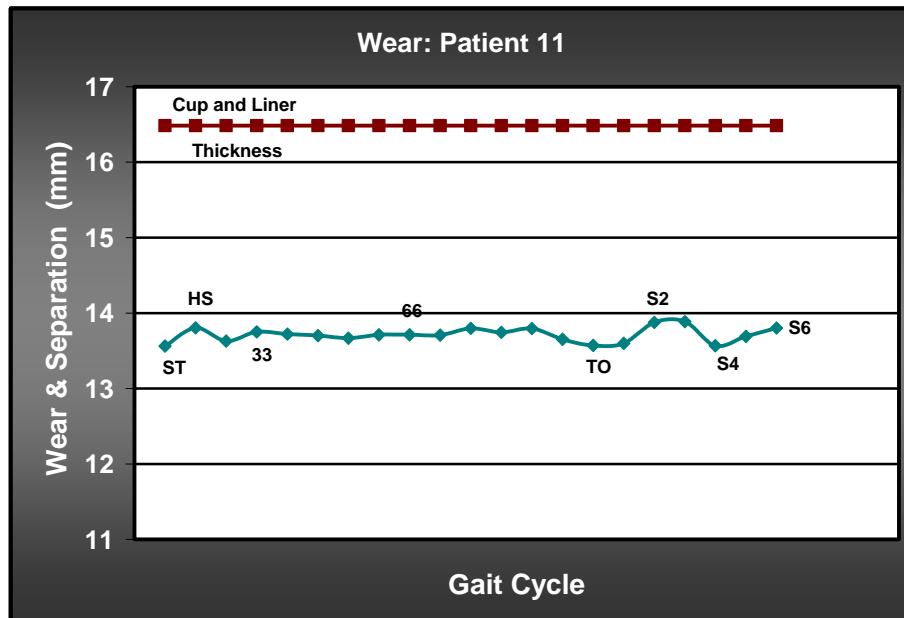
Figure 17: (Top) Excessive Wear Subject, (Bottom) A Subject with No Wear and No Separation Subject
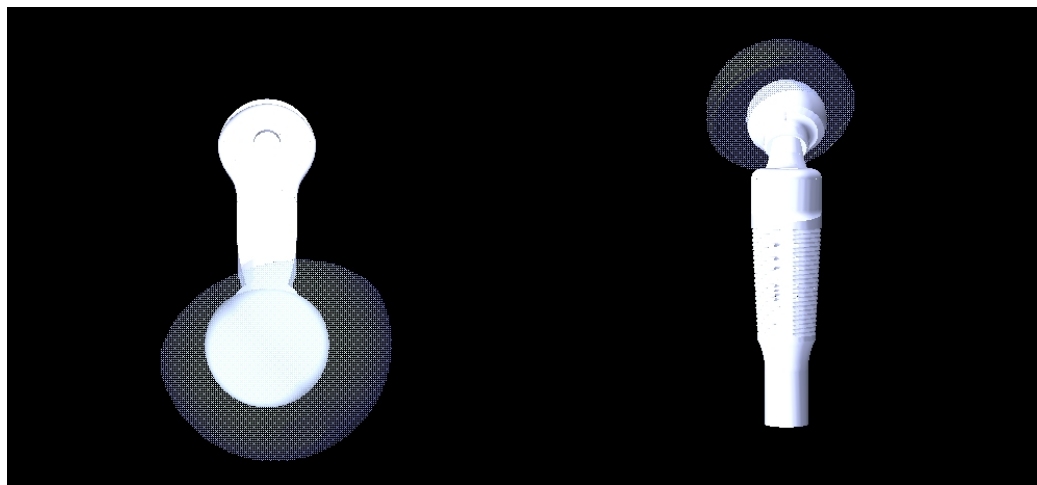
Figure 18: Implant Overlays of Subject with Femoral Edge Loading (Left) Top View, (Right) Back View

This caused excessive sliding distance values in comparison to the subject liner thickness values (Figure 19).

During the gait phase evaluations, twelve subjects experienced femoral head separation from the acetabular shell. These values were then compared with post-operative times. The incidence of separation was deemed to be statistically significant for this study. However the correlation of post-operative times with separation was found to be insignificant once again. The threshold for femoral head separation during gait was 0.56 mm. The maximum value of separation found was approximately 3.5 mm (Figure 20). A comparison of the maximum separating subject with a non-wear, non-separating subject can be seen in Figure 21. The subject with the maximum femoral head separation subject
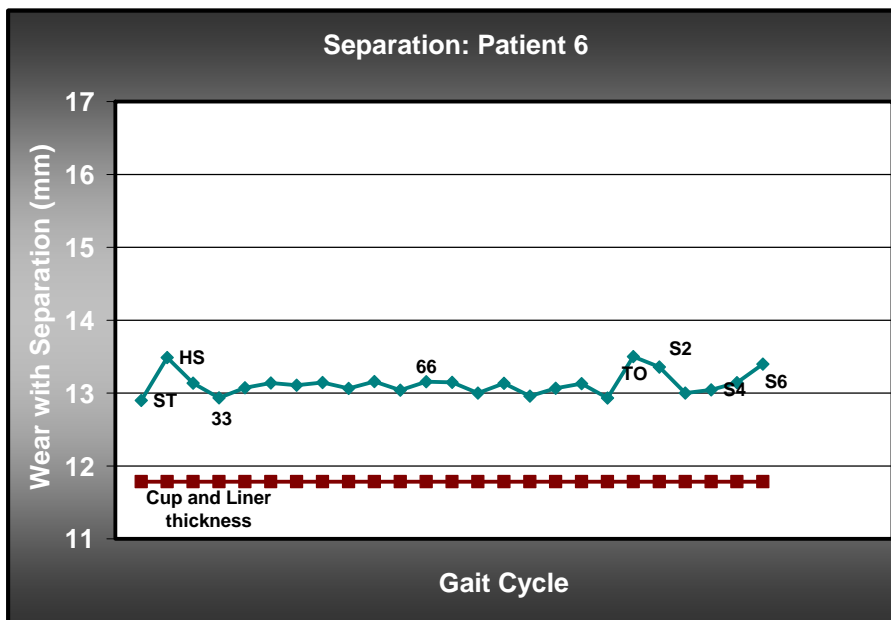
Figure 19: Subject with Negative Wear Values throughout Gait Cycle Predicting Femoral Edge Loading
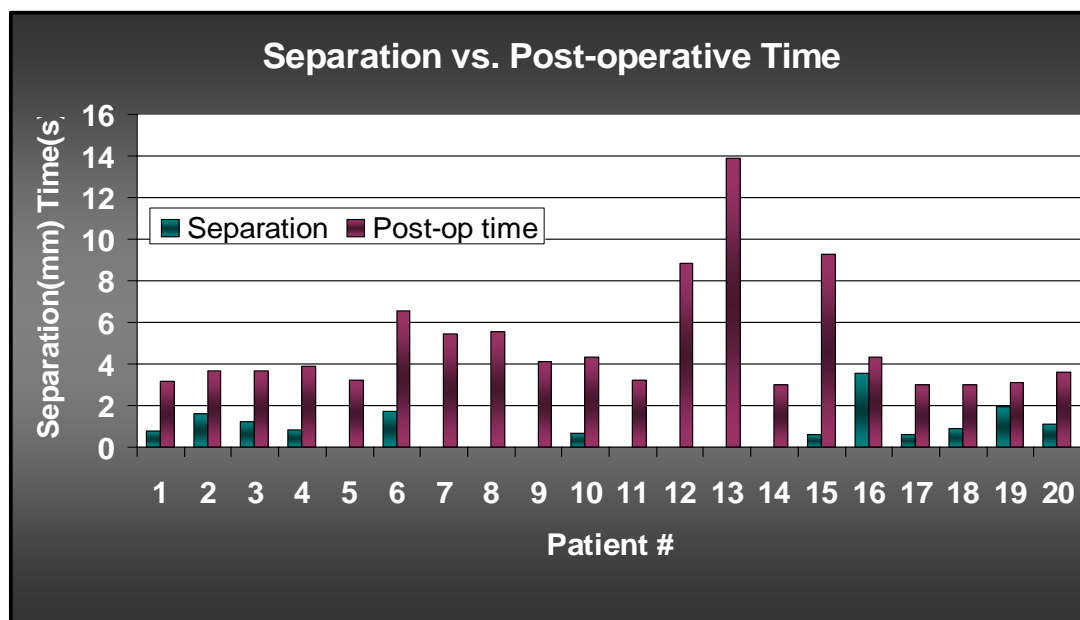

Figure 20: Separation vs. Post-operative Times for All Twenty Subjects
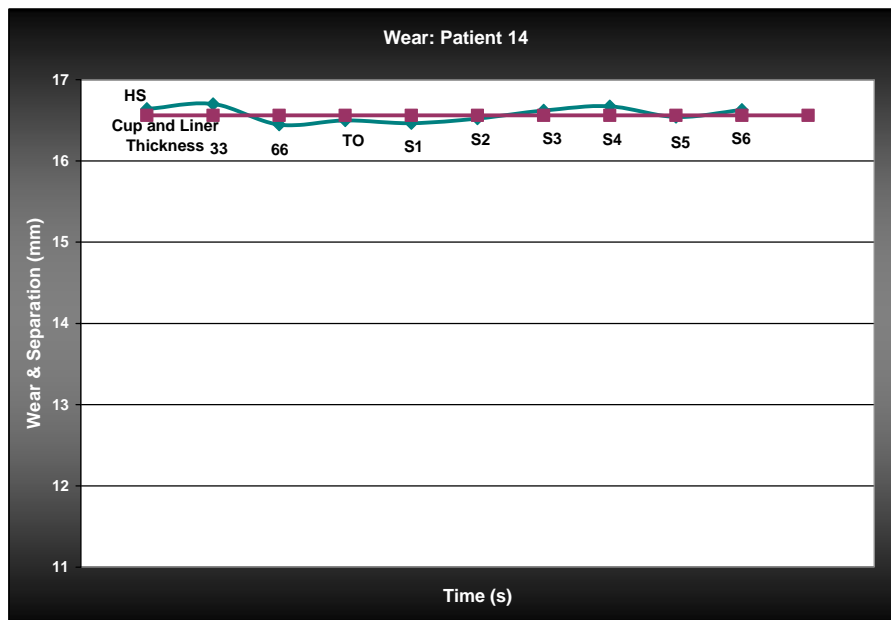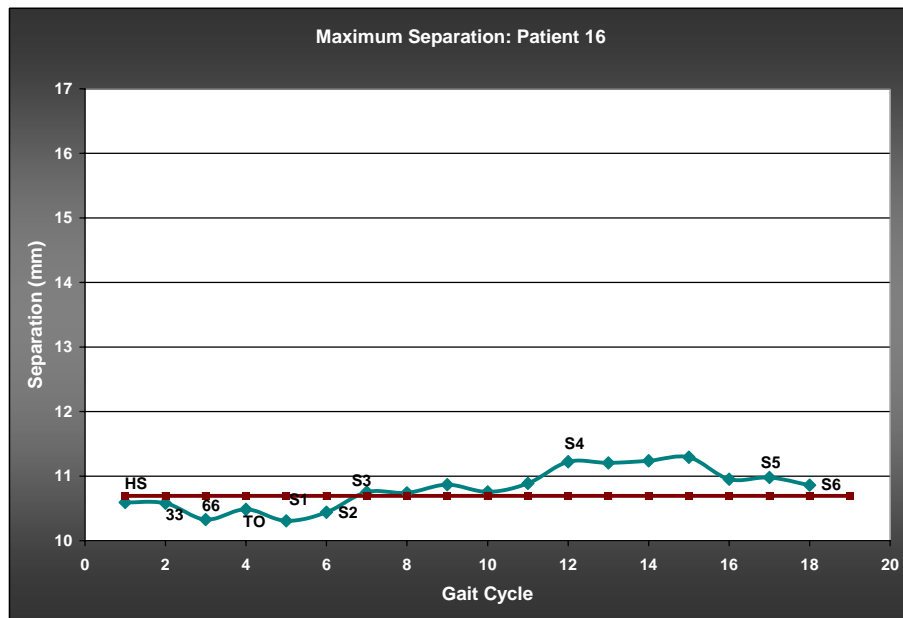
Figure 21: (Top) Femoral Edge Loading (Bottom) A Subject Experiencing No Wear, and No Separation

was also determined to have approximately 0.4 mm of wear.

Separation was found to occur most often around 66% of the gait cycle, either from the transition of 33%-66% gait or from 66%-gait to toe-off (approximately 50% of separators). Twenty-five percent of separators experienced separation during swing phase and the other twenty-five percent exhibited signs of never being fully seated in their acetabular shell as mentioned earlier. Ten percent of the group demonstrated both separation and wear (Figure 22).

3.2 Kinematic and Kinetic Analysis

Initial kinetic analysis was performed on two subjects: one subject, a male, with 0.63 mm of separation and no wear (subject A), and one subject, a female, experiencing 0.56 mm wear but no separation (subject B). Rotation and translation data was transformed into simple polymertric equations (Figure 23 & 24). There were definite differences between the kinematics experienced by the two subjects. Subject A had a stride time of 2.06 seconds with stance phase (toe-off) ending at 1.46 seconds. Subject B had a shorter full stride time of 2.03 seconds, but a longer stance phase (toe-off) ending at 1.83 seconds into the stride. Rotations of subject A are much larger in range than subject B which may be due to the longer stride time. Subject A also had a negative range of translations whereas subject B's translations are all mostly positive. Predicted force profiles of subjects A and B were similar in shape and magnitude with variations only appearing in the time differences that each subject took to perform one stance-phase
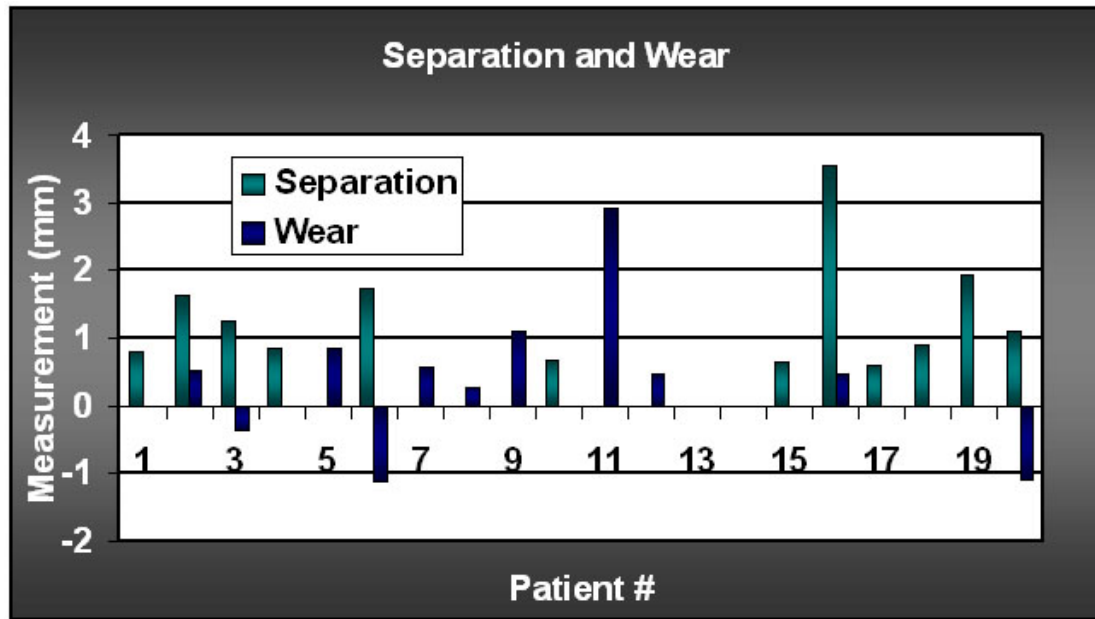
Figure 22: Graph of Separation and Wear
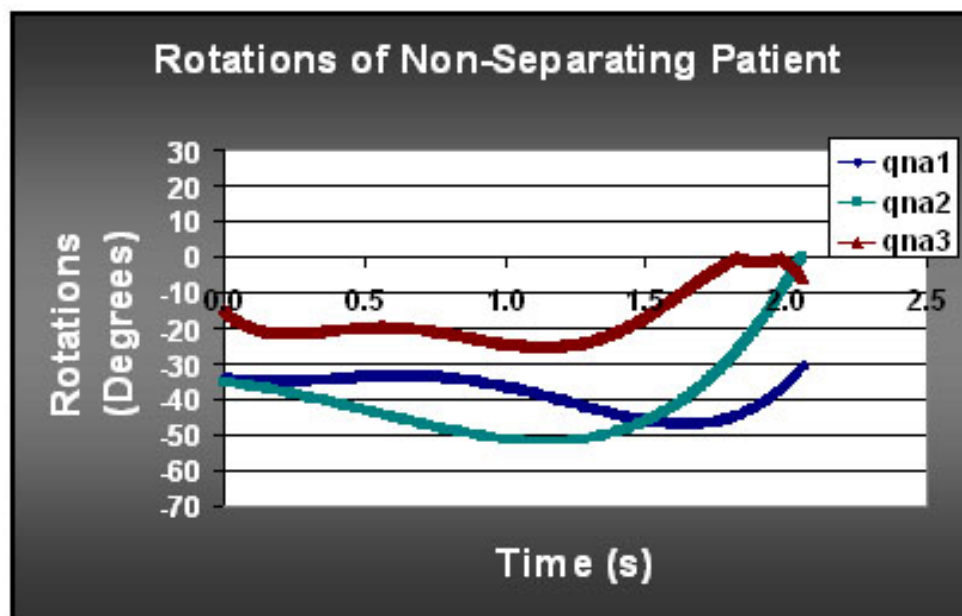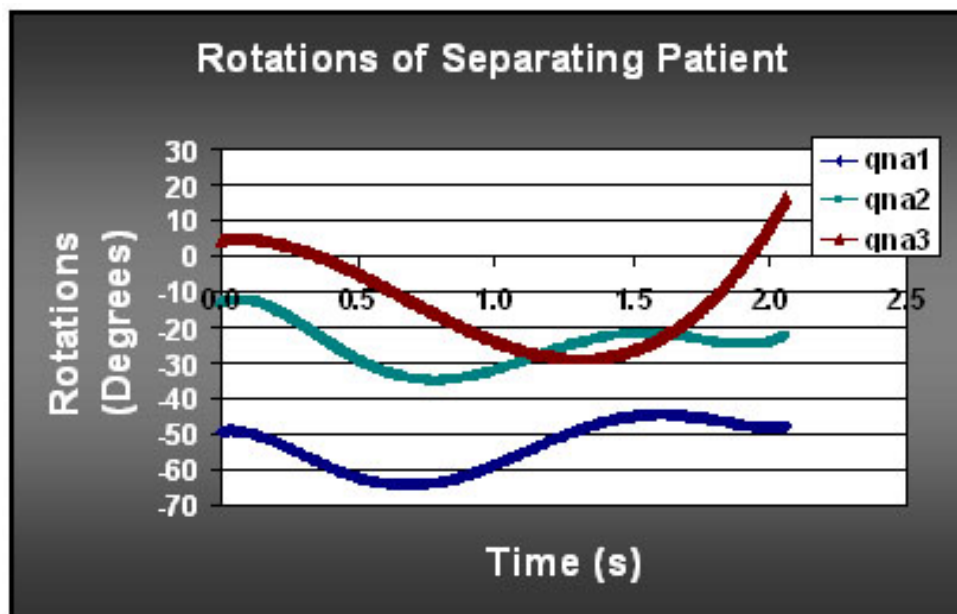
Figure 23: Rotations of Subjects (Top) Subject A and (Bottom) Subject B
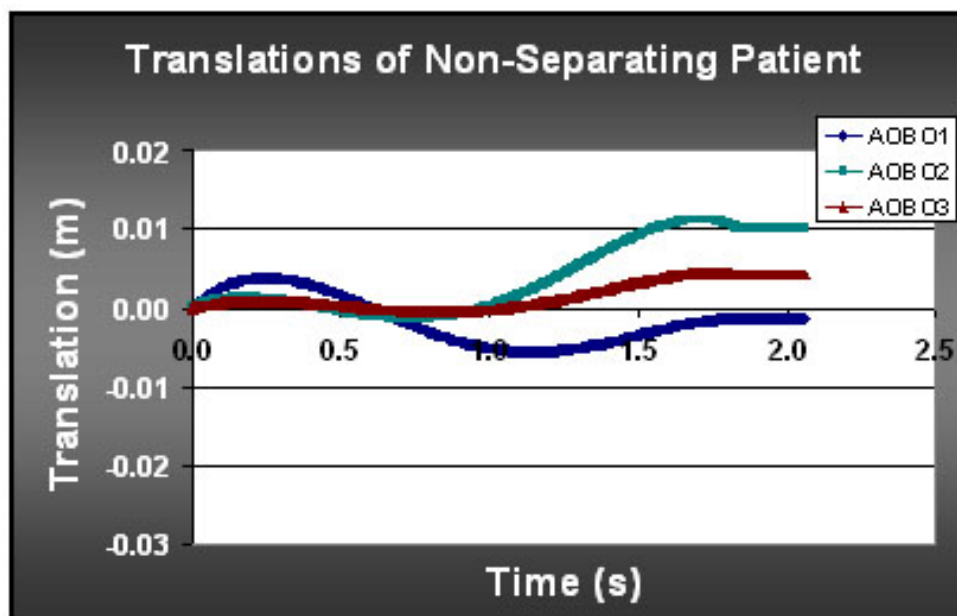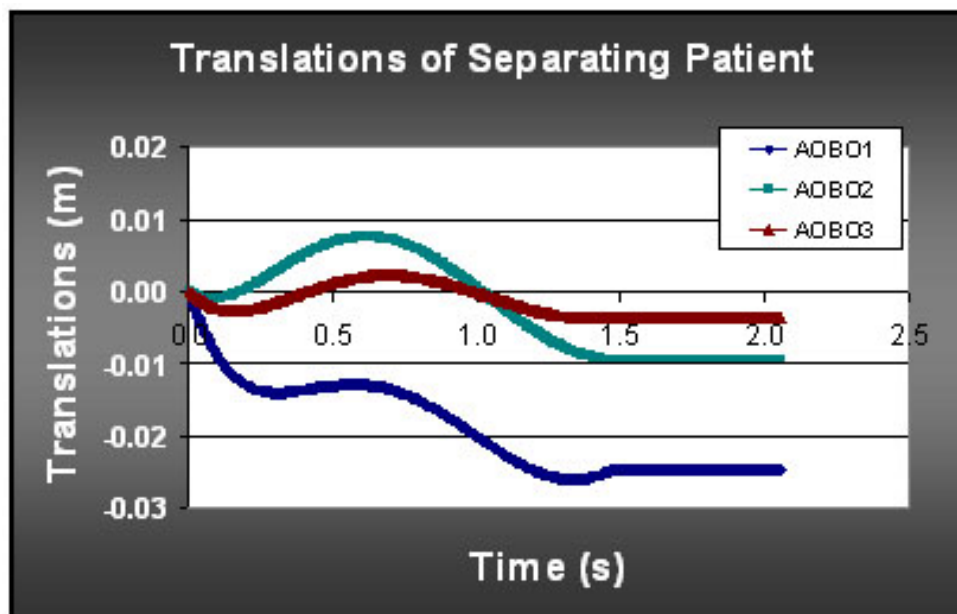
Figure 24: Translations of Subjects (Top) Subject A and (Bottom) Subject B

of gait (Figure 25 & 26). The maximum vertical force at the hip joint for subject B was found to be approximately 1.75 times body weight, occurring at 66% of the gait cycle. The vertical hip joint force for subject A was slightly higher at approximately 1.9 times body weight, also occurring near 66% of the gait cycle (Figure 27). Boundary forces between the vertebral body L5 and the pelvis produced a similar trend with 1.8 times body weight for subject A and 1.75 times body weight for subject B (Figure 28-30). Torques at the hip joint and back were also higher in subject A in the horizontal (N1>) direction (Figure 31-34).
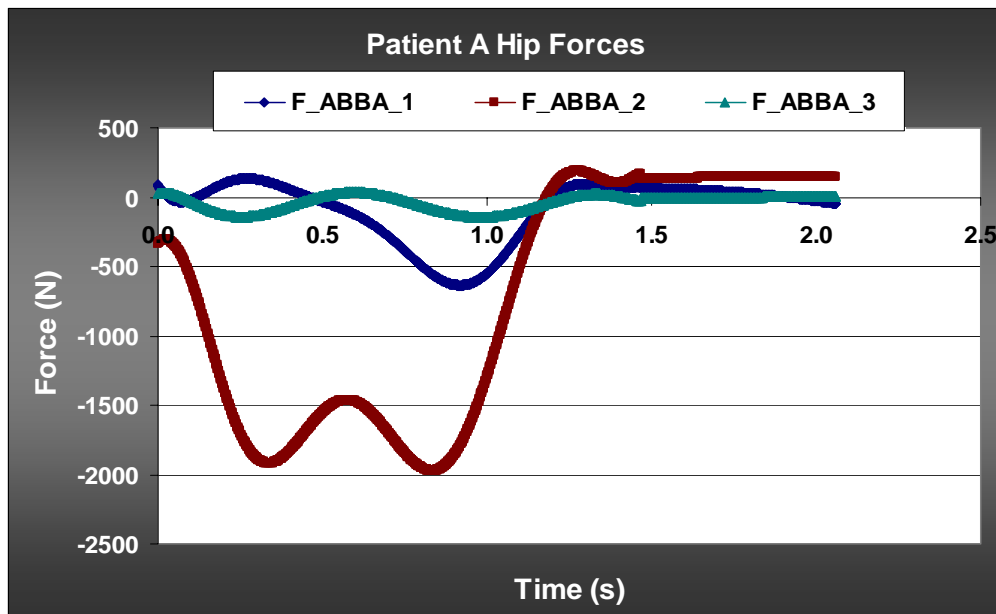
Figure 25: Hip Joint Forces for the Separating Subject
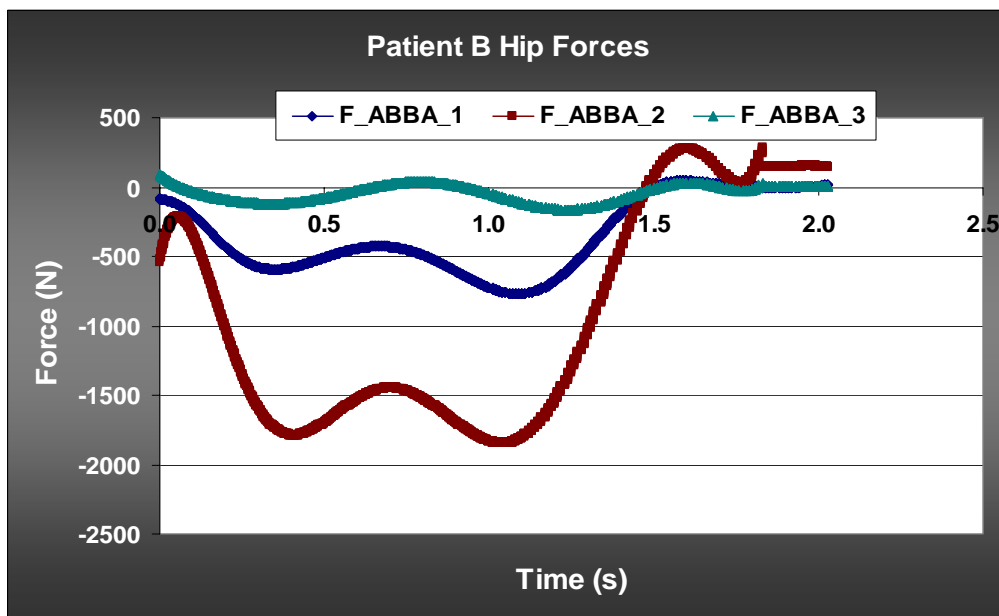
Figure 26: Hip Joint Forces for the Wear Subject
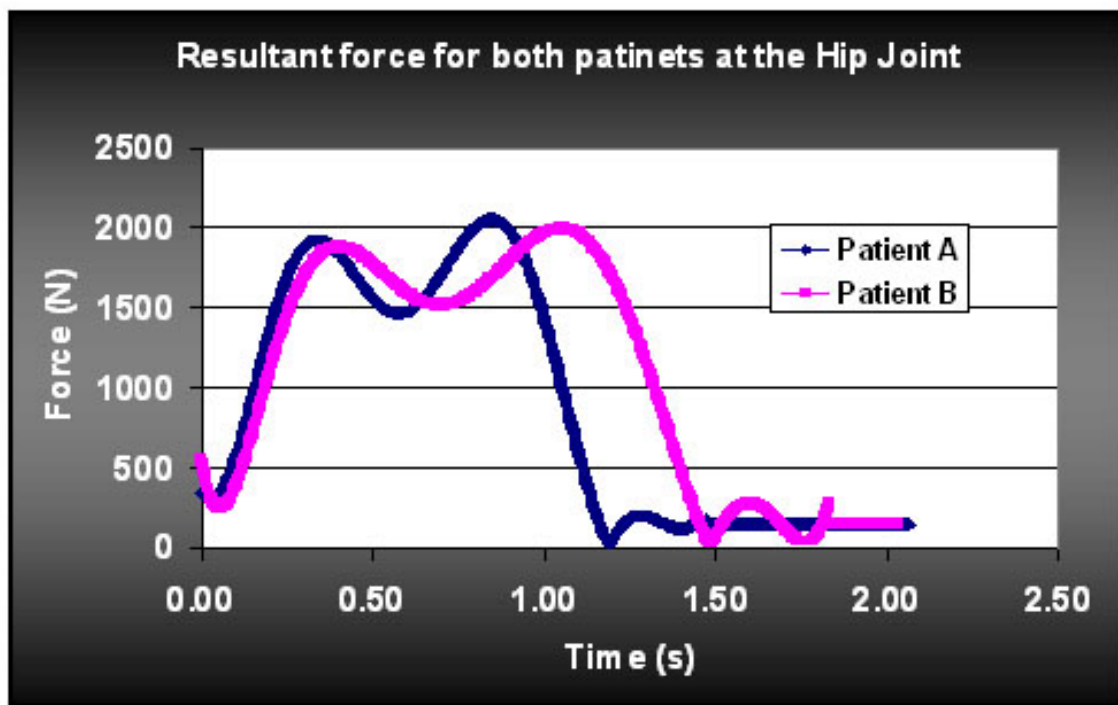
Figure 27: Resultant Forces for Subject A and B at the Hip Joint
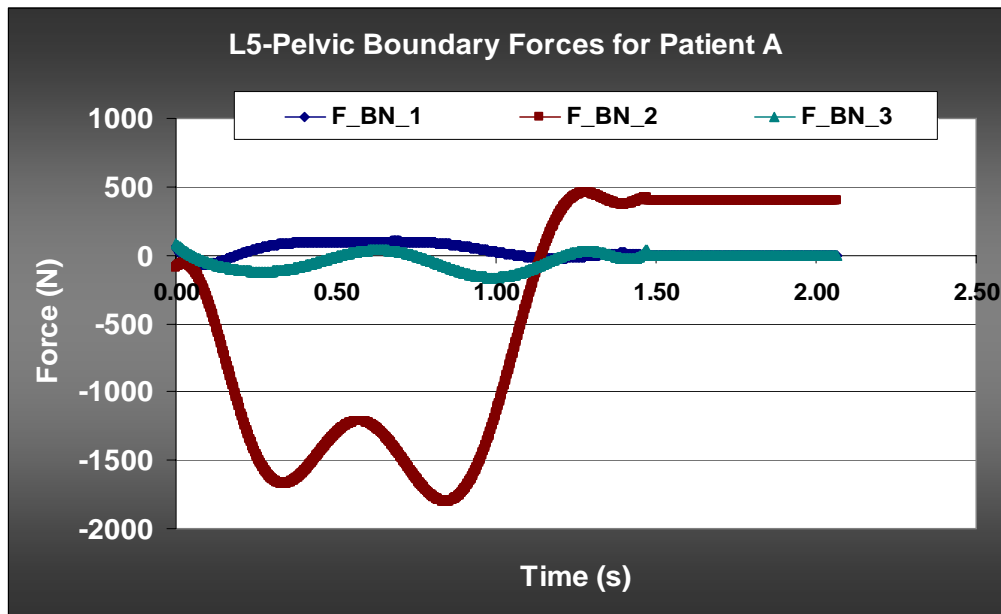
Figure 28: L5-Pelvic Boundary Forces for Subject A
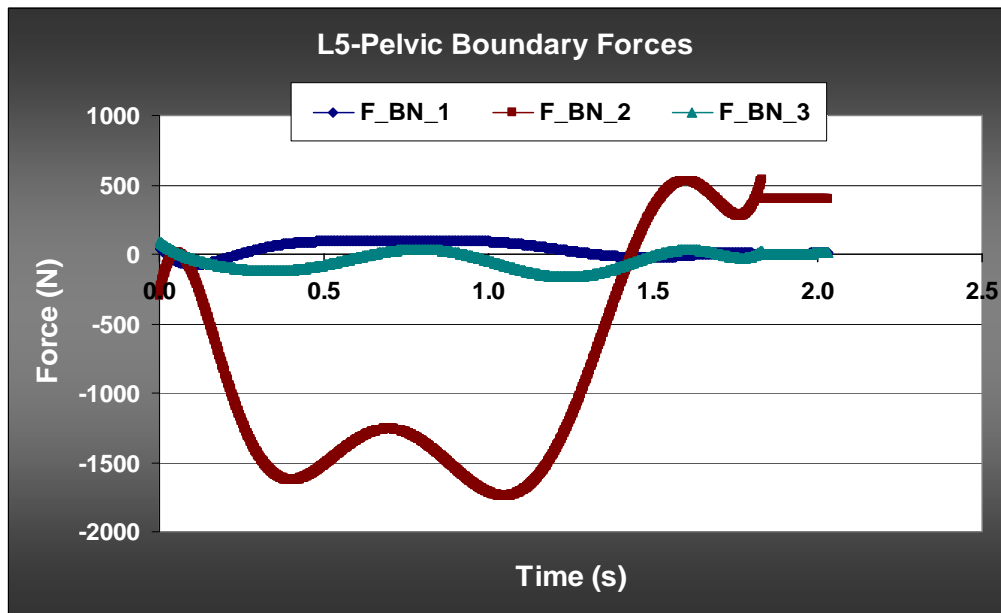
Figure 29: L5-Pelvic Boundary Forces for Subject B
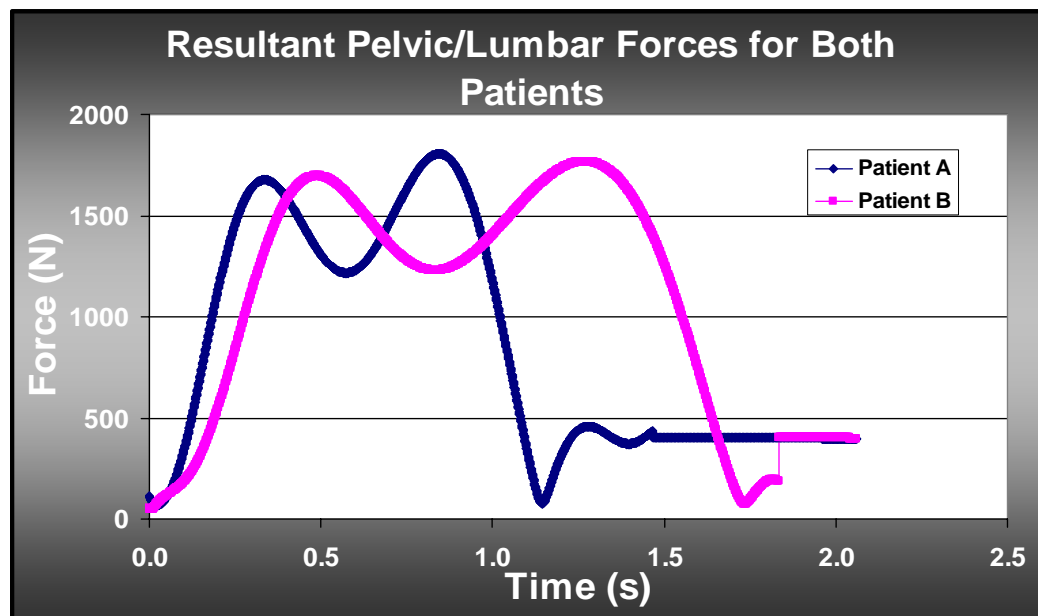
Figure 30: Resultant Forces for L5-Pelvic Boundary Forces of Both Subjects
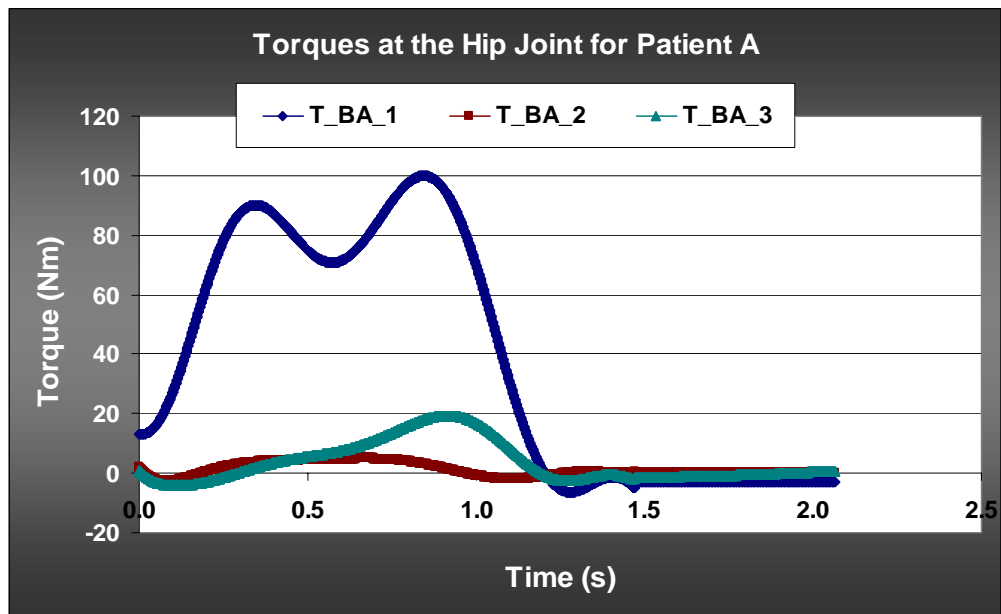
Figure 31: Torques at the Hip Joint for the Subject A
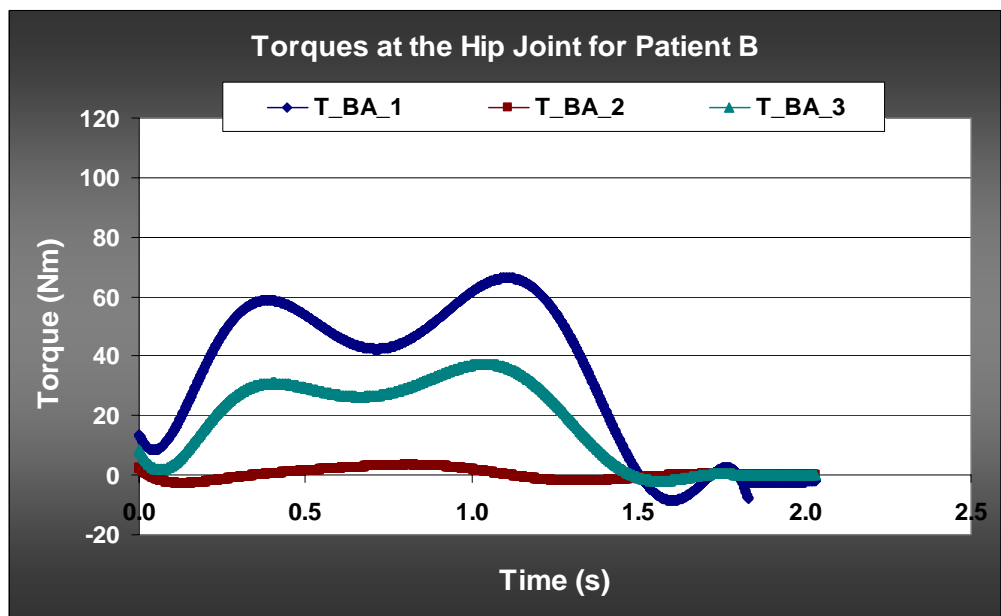
Figure 32: Torques at the Hip Joint for Subject B
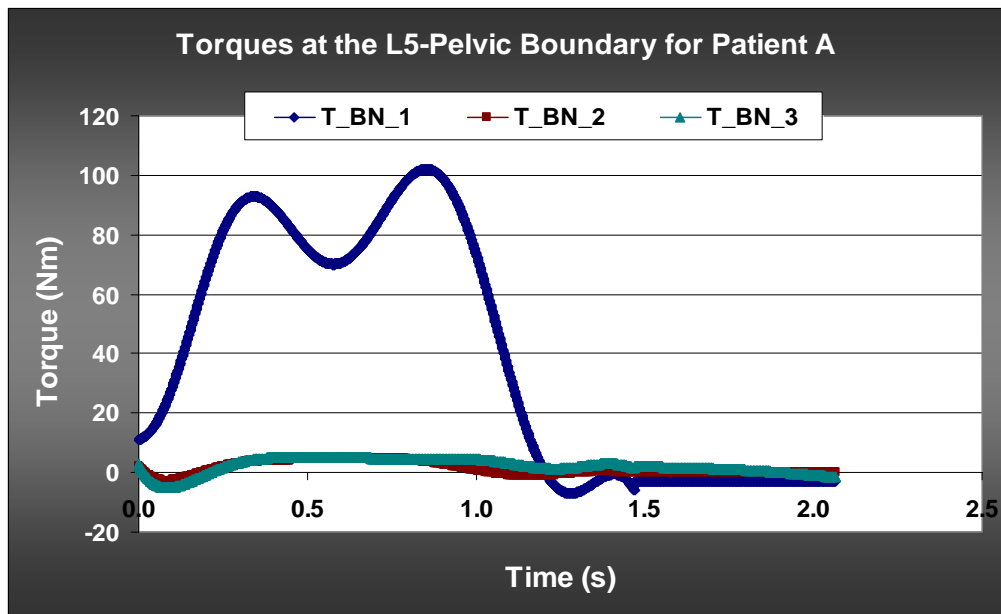
Figure 33: Torques at the L5-Pelvic Boundary for Subject A
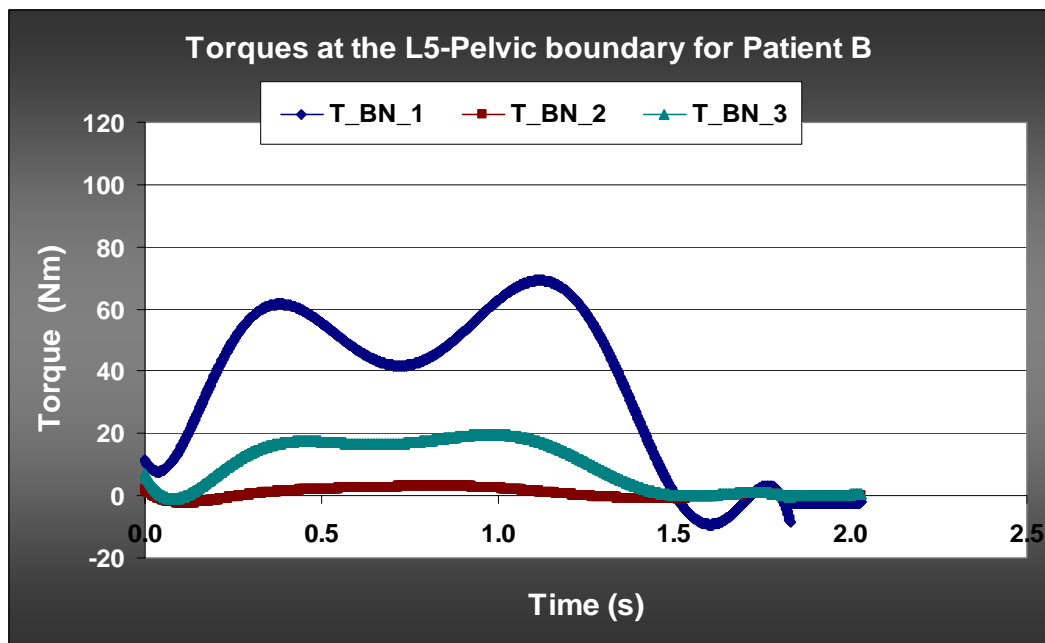
Figure 34: Torques at the L5-PelvicBboundary for Subject B

Chapter 4

Discussion

4.1 Discussion

A summary of the 2-D to 3-D analysis can be studied in Figure 35. Statistical correlations were made separately using one-sample t-test for wear and for separation, as well as a Spearman's rho correlations test between wear, separation, and post-operative times (Table 2). Using the one-sample t-test with a 95% confidence interval for separation, values in the study were found to be significant with a p-value of 0.001. Data correlation using the Spearman's rho test between separation, wear, and post-operative time indicated a very strong negative correlation between wear and separation. Correlations between post-operative times and separation were found to be slightly negative, but over all insignificant. Correlations between post-operative times and wear are positive, but also insignificant.

The most interesting and unexpected finding with the statistical analysis was that correlation between separation and wear was determined to be a negative correlation (Table 2). This informed us that separation was not necessarily causing wear in this subject group. The original hypothesis to this study was that greater separation between

Normal
14%

wear
32%

sep
54%
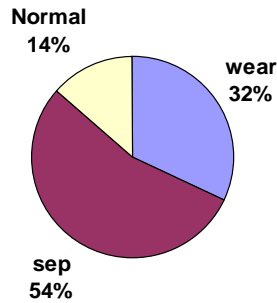
Figure 35: Chart of 2-D to 3-D Analysis Outcome

Table 2: Data Correlations Found by Spearman's Rho Test

Correlations			Separation	Wear	Post-Operative Time
Spearman's Rho	**Separation**	**Correlation Coefficent**	**1.000**	**-0.499***	**-0.156**
		Sig. (2-tailed)		**0.025**	**0.512**
		N	**20**	**20**	**20**
	Wear	**Correlation Coefficent**	**0.499***	**1.000**	**0.047**
		Sig. (2-tailed)	**0.025**		**0.843**
		N	**20**	**20**	**20**
	Post-Operative Time	**Correlation Coefficient**	**-0.156**	**0.047**	**1.000**
		Sig. (2-tailed)	**0.512**	**0.843**	
		N	**20**	**20**	**20**

* Correlation is significant at the 0.05 level (2-tailed).

the femoral head and acetabular components would cause more of an impact force on the acetabular liner, and alter natural movement, therefore causing more wear. An explanation for negative correlation between separation and wear may be that that the subjects not experiencing femoral head separation were implanted more tightly leading to increased bearing surface forces that may have lead to increased wear. Wear can also be caused by a variety of factors including subject activity and polyethylene pre and post-processing. A study comparison on subject activity and processing of the different liner types might be useful in determining causes of wear in the current study.

Using the kinetic solutions between a subject with separation values and one with wear values, higher forces were seen in the subject with separation. This matches the original hypothesis in that the phenomenon of separation causes an impact loading force and therefore increasing the forces between the femoral head and acetabulum. A new formulated theory then may be that the tighter implantation of the THA may lead to increased wear of the polyethylene insert caused by the higher contact forces. It is also possible however, that separation may be allowing synovial fluid to enter between the femoral head and acetabular shell therefore allowing a protective layer to form over the polyethylene reducing wear. Further long term follow-up studies may need to be performed with a group of subjects from directly post operative through wear and implant failure to determine if wear could be a determinate factor for separation. And of course for an overall better view of the current project's kinetic comparison, more subjects

would need to be analyzed for kinematics and kinetics as well as more images analyzed during the gait cycle for increased exactness in equation modeling.

Another interesting observance was the higher torque values predicted in this study, which may be directly related to the simplicity of this model. In the human body, the muscle forces influence motion in the human body, including the rotations that occur between to subsequent bones. In the human body, muscles can also restrict the motion leading to a more natural motion that may have moments, but not necessarily a torque. Without those muscles and other soft-tissue constraints we essentially are modeling a motor at each joint to product the rotations. Without resistive structures, the torques required to produce the motions normally activated by the muscles, may be higher than one would expect. In the future modeling for this project, we will add in soft-tissue structures, which may reduce the applied torques in this system.

Chapter 5

Conclusion and Future Considerations

5.1 Conclusion and Future Considerations

Separation was determined to occur significantly in subjects with MOP THA implants. However, why it occurred and what problems it may have caused to the individuals are still unknown. The current study has shown that wear and separation are negatively correlated. It has also shown that higher forces occurred for a subject with separation compared to a subject without separation. However, the current theoretical modeling method only considers the bodies of the femur and the pelvis with no muscle forces included. A literature search, using Gray's Anatomy text and an interactive anatomy software, Primal StudiosTM, was performed during the early stages of the current project to find muscles at the hip joint active during gait. The muscles and ligaments were then divided into six groups as tabulated in Table 3. Force profiles of the chosen muscles would need to be determined through cadaver testing, literature, or through the use of imaging techniques of live subjects.

Loci tracking involves computer placement of points on the femoral head and tracks their location during the analysis. This tracking creates a graphical path of the

Table 3: Table of Muscles used During Gait and Their Groupings Due to Their Actions

Rotation	Muscles
Lateral Rotation	Gamellus (superior/inferior), Obturator (External/Internal), Piriformis, Quadratus Femoris, Gluteus Maximus/Medius
Medial Rotation	Gluteus Minimus, Tensor Fascia Lata
Flexion	Gracilis, Sartorius, Tensor Fascia Lata, Illiopsoas
Extension	Biceps Femoris, Rectus Femoris
Abduction	Gluteus Minimus/Medius
Adduction	Adductor Longus/Magnus/Brevis, Gracilis

specified points during the movement which may or may not increase the current models sensitivity. (Mahfouz 2003, Turell 2003)

Researchers have also previously suggested that the (American Academy of Orthopedic Surgeons 2005), the position of the acetabular shell component be defined more accurately and used as input to the parametric model. Multiple studies have been done on the effect of the shell placement and the kinematics of the THA implanted hip. It has been found in these studies that dislocation and wear may occur more often with some combinations of acetabulum shell orientation angles.(Widmer 2003, Bourne 2004, Pietrabissa 1998) Surgeons are interested to know if, with this current study, the shell placement might also have a role in separation and/or increased forces at the hip joint. Additions to the current study are a continuously growing list. In the current study separation was found to occur significantly in MOP subjects and have a negative correlation with wear. The kinetic analysis of the separation subject also produced higher forces at the hip joint showing signs of possible impulse loading. However, the answer to the questions of why separation occurs and to what effect it has on the THA implant and kinematics of the subject are still undetermined. Future studies will involve advancement of the present model to incorporate more clinical information and the implementation of soft-tissue

REFERENCES

References – Websites

AAOS "*Improving Musculoskeletal Car in America: Osteoarthritis of the Hip: Joint Replacement*" visited on 02-05-05
  Link: www.aaos.org Rosemont, IL 2003

Mathworks. "*ToolBox*". Visited on 04-1-2005.
  Link:
  http://www.mathworks.com/access/helpdesk/help/toolbox/physmod/mech/mech_studies3.html 2005

Stryker. "*Patient Labeling Information*". Visited on 04-1-05
  Link: http://www.strykerceramics.com/stryker/labeling.php

References – Publications

Bergman G, F Graichen, A Rohlmann, HL Linke, 1997: "*Hip joint forces during load carrying*". Clinical Orthopedics 335, 190-201

Bergman, G, F Graichen, A Rohlmann, 1993: "*Hip Joint Loading During Walking and Running, Measured in Two Subjects*". Journal of Biomechanics 26, 969-990

Bergman, G., G. Deurtzbacher, M. Heller, F. Graichen, A. Rholmann, J. Strauss, G.N. Duda, 2001: "*Hip Contact Forces and Gait Patterns from Routine Activites*". Journal of Biomechanics 34, 859-871

Bourne, R., M.D., FRCSC, R Mehin, MD, FRCSC, 2004: "*The Dislocating Hip What to Do, What to Do*". Journal of Arthroplasty 19, 4

Brand, R.A., R.D. Crownsheild, C.E. Wittock, 1982: "*A Model of Lower Extremity Muscular Anatomy*". Journal of Biomechanics 104, 304

Brand, R.A., D.R. Pedersen, D.T. Davy, G.M. Kotzar, K.G. Heiple, V.M. Goldberg, 1994: "*Comparison of Hip Force Calculations and Measurements in the Same Subject*". Journal of Arthroplasty 9 45-51

Cappazzo, A, 1991: "*Three-Dimensional Analysis of Human Walking: Experimental Methods and Associated Artifacts*". Human Movement Science 10 589-602

Cheze, L, 2000: "*Comparison of Different Calculations of Three-Dimensional Joint Kinematics from Video-Based System Data*". Journal of Biomechanics 33 1695-1699

Cianci, R., F. Baruffaldi, F. Fabbri, S. Affatato, A. Toni, A. Giunti, 1995: "*A Computerized System for Radiographical Evaluation in Total Hip Arthroplasty*". Computer Methods and Programs in Biomedicine 46 233-243

Clarke, I.C., V. Good, L. Anissian, A. Gustafson, 1978: "*Charnley Wear Model Validation of Hip Simulators-Ball Diameter Versus Polytetrafluoroethylene and*

Polyethylene Wear". Proceedings of the Institute of Mechanical Engineers 211 (1), 25-36

Crowninsheield, R.D, 1978: "*Use of Optimization Techniques to Predict Muscle Forces*". Journal of Biomechanical Engineering 100, 88-92

Crowninsheield, R.D., R.C. Johnson, J.G. Andrews, R.A. Brand, 1978: "A *Biomechanical Investigation of the Human Hip*". Journal of Biomechanics 11 75-85

Davy, DT, GM Kotzar, RH Brown, KG Heiple, VM Goldberg, KG Heiple Jr., J Berilla, AH Burstein, 1988: "*Telemetric Force Measurements Across the Hip After Total Arthroplasty*". Journal of Bone and Joint Surgery America 70 45-50

De Lange, A., R. Huiskes, J.M.G. Kauer, 1990: "*Measurement Errors in Roentgen-Stereophotogrammetric Joint-Motion Analysis*". Journal of Biomechanics 22 259-269

D'Lima DD, Townsend CP, Arms SW, Morris BA, Colwell CW Jr., 2005: "*An Implantable Telemetry Device to Measure Intra-Articular Tibial Forces*". Journal of Biomechanics 38, 299-304.

English, TA, 1978: "*Measurement of Hip Load Forces In Vivo using a Telemetric Method Design, Method and Results*". British Orthopedic Research Society, Bradford, England

Fisher .(verbal conversation with Dr. John Fisher, Leeds University England)

Fuller, J., L. J. Liu, M. C. Murphy, R. W. Mann, 1997: "*A Comparison of Lower Extremity Skeletal Kinematics Measured using Skin- and Pin-Mounted Markers*". Human Movement Science 16 219-242

Glyn-Jones S., Gill, H.S., Mclardy-Smith P., Murray D. W, 2004: "*Roentgen Stereophotogrammetric Analysis of the Birmingham Hip Resurfacing Arthroplasty: A Two-Year Study*". Journal of Bone and Joint Surgery

Hof, A.L., E. Otten, 2004: "*Assessment of Two-Dimensional Induced Accelerations from Measured Kinematic and Kinetic Data*". Gait and Posture Article in Press

Hopper, R.H., Jr., PhD, A.M. Young, MS, K.F. Orishimo, MS, J.P. McAuley,

MD "*Correlation Between Early and Late Wear Rates in Total Hip Arthroplasty with Application to the Performance of Marathon Cross-linked Polyethylene Liners*". Journal of Arthroplasty 18 (7)

Huston, Ronald L., 1990: Multibody Dynamics. Butterworth-Heinemann, Stoneham, MA USA

Jalali-Valhid, D., M. Jagatia, Z.M. Jin, D. Dowson, 2004: "*Prediction of Lubricating Film Thickness in UHMWPE Hip Joint Replacements*". Journal of Biomechanics 34 261-266

K., Thomas, D.A. Levinson, 2000: Dynamics Online: Theory and Implementation with Autolev^{TM}, Online Dynamics, Inc, Sunnyvale, CA.

Komistek, R.D., PhD, D.A. Dennis, MD, J.A. Ochoa, PhD, B.D. Haas, MD, C. Hammill, BS, 2002: "*In Vivo Comparison of Hip Separation after Metal-on-Metal or Metal-on-Polyethylene Total Hip Arthroplasty*". Journal of Bone and Joint Surgery

Komistek, R.D., PhD, J.B. Stiehl, D.A. Dennis, R.D. Paxsonn, R.W. Soutas Little, 1988: "*Mathematical Model of the Lower Extremity Joint Reaction Forces using Kane's Method of Dynamics*". Journal of Biomechanics 31 185-189

Leva, P, 1996: "*Adjustments to Zatsiorksy-Seluyanov's Segment Inertia Parameters*". Journal of Biomechanics 29 (9) 1223-1230

Madsen, M.S. Ritter, M.A. Morris, H.H. Meding, J.B. et al., 2004: "*The Effect of Total Hip Arthroplasty Surgical Approach on Gait*". Journal of Orthopedic Research 22 44-50

Masao, A., MD, T. Nonaka, MD, F. Nishisaka, MD, S. Mori, MD, K. Fukuda, MD, C. Hamanishi, MD, PhD, 2004: "*Late Dissociation of an Alumina-on-Alumina Bearing Modular Acetabular Component*". Journal of Arthroplasty 19

Mahfouz, M., W. Hoff, R. Komistek, and D. Dennis, 2003: "*A Robust Method for Registration of Three-Dimensional Knee Implant Models to Two-Dimensional Fluoroscopy Images*". IEEE Trans. Medical Imaging 22 1561-74, 2003.

McKellop, H.A., P. Campbell, S.H. Park, T.P. Schmalzried, P. Grigoris, , H.C. Amstutz, A. Sarmiento, 1996: "*The Origin of Submicron Polyethylene Wear Debris in Total Hip Arthroplasty*". Clinical Orthopedics 311 3-21

McKellop, H.A., I.C. Clarke, "*Evolution and Evaluation of Materials-Screening Machines and Joint Simulators in Predicting In Vivo Wear Phenomena*." In Duchyene, P. Hastinkg, G.W. (Eds.), <u>Functional Behavior of Orthopedic Biomaterials Applications, Vol. II</u> . CRC Press Boca Raton, FL, 51-85

McKellop, H.A., B. Lu, P. Benya, 1992: "*Friction , Lubrication and Wear of Cobalt Chromium, Alumina and Zirconia Hip Prosthesis Compared on a Joint Simulator*". Proceedings of the 38th Annual Meeting of the Orthopedic Research Society, Washington D.C. 356

McKellop, H.A., B. Lu, S. Li, 1992: "*Wear of Acetabular Shells of Conventional and Modified UHMW Polyethylene Compared on a Hip Joint Simulator*." Proceedings of the 38th Annual Meeting of the Orthopedic Research Society, Washington D.C.

McKellop, H.A., T. V. Rostlund "*The Wear Behavior of Ion-Implanted Ti-6Al-4V against UHMW Polyethylene*". Journal of Biomedical Materials and Research 24, 1413-1425

Muratoglu, O.K., PhD, C.R. Bragdon, BS, D. O'Conner, AS, R.S. Perinchief, BS, D.M. Estok II, MD, M. Jasty, MD, W.H. Harris, MD, 2001: "*Larger Diameter Femoral Heads Used in Conjunction with a Highly Cross-Linked Ultra High Molecular Weight Polyethylene*". Journal of Arthroplasty 16 (6) 24-30

Nevelos, J., PhD, E. Ingham, PhD, C. Doyle, PhD, R. Streicher, PHD, A. Nevelos, FRCS, W. Walter, FRACS, j. Fisher, D Eng, 2000: "*Microseparation of the Centers of Alumina-Alumina Artificial Hip Joints During Simulator Testing Procedures Clinically Relevant Wear Rates and Patterns*" Journal of Arthroplasty 15 (6)

Norkin, C.C., Levangie, P.K., 1983: <u>Joint Structure and Function A Comprehensive Analysis</u>. F.A. Davis Company, Philadelphia, PA, 1983

Outten, J. 2005: "*A Computational Model to Predict In vivo Lower Limb Kinetics and Assess Total Knee Arthroplasty Design Parameters*" <u>Thesis</u>, University of Tennessee Knoxville

Ostgaard, S.E., L. Gottlieb, S. Toksvig-Larsen, A. Lebech, A. Talbot, B. Lund, 1997: "*Rontgen Stereopphotogrammetric Analysis using Computer-Based Image-Analysis*" Journal of Biomechanics Vol 30. 9 993-995

Pietrabissa, R., R. Manuela, D.M. Elina, 1998: "*Wear of Polyethylene Shells in Total Hip Arthroplasty: A Parametric Mathematicial Model*" Medical Engineering & Physics 20 199-210

Radetsky, P., 1986: "*The Man Who Mastered Motion*". Science May 44-52

Ramamaurti, B.S., C.R. Bragdon, D.O. O'Conner, J.D. Lowenstein, M. Jasty, D.M. Estok, W.H. Harris, "*Loci of Movement of Selected Points on the Femoral Head During Normal Gait. Three-Dimensional Computer Simulation.*" Journal of Arthroplasty 11 (7) 845-852

Saikko, V.O., P.O. Paavolainen, P. Slatis, 1993: "*Wear of the Polyethylene Acetabular Shell. Metallic and Ceramic Heads Compared in a Hip Simulator*". Acta Orthopedic Scandinavica 64(4) 391-402

Sati, M., J. A. de Guise, S. Larouche, G. Drouin, 1996: "*Quantitative Assessment of Skin-Bone Movement at the Knee*". The Knee 3(3) 121-138

Schinsky, M.F. Nercessian, O.A. Arons, R.R. and Macaulay, W., 2003: "*Comparison of Complications After Transtrochanteric and Posterolateral Approaches for Primary Total Hip Arthroplasty*". Journal of Arthroplasty 18, 430-434

Sharma, Adrija, 2005: "*A Method to Calculate the Femoro-polyehtylene Contact Pressures in Total Knee Arthroplaty In-Vivo*". <u>Thesis</u>, University of Tennessee Knoxville

Slevick, G., 1989: "*Roentgen Stereophotogrammetry. A Method for the Study of the Kinematics of the Skeletal System*". Acta orthopedica Scandinavica Suppliments 232, 1-51

Sovai, R., M. Motta, A. Visani, 1999: "*Variation of the Spatial Position Computed by Roentgen Stereophotogrammetric Analysis (RSA) under Non-Standard Conditions*" Medical Engineering and Physics 21 575-581

Stansfield, B.W., A.C. Nicol, 1998: "*Hip Joint Force in 40-60 Year Olds During Activities of Daily Living*" 11thconference of the ESB, July 8-11, Toulouse, France

Stansfield, B.W., A.C. Nicol, 2002: "*Hip Joint Contact Forces in Normal*

Subjects and Subjects with Total Hip Prostheses: Walking and Stair and Ramp Negotiation". Clinical Biomechanics 17 130-139

Stewart, T.D., PhD, J.L. Tipper, PhD, G. Insley, PhD, R.M. Streicher, PhD, B. Ingham, PhD, J. Fisher, PhD, 2003: "*Severe Wear and Fracture of Zirconia Heads Against Alumina Inserts in Hip Simulators with Microseparation*". Journal of Arthroplasty 19 (6)

Taylor, SJ, JS Perry, JM Meswania, N Donaldson, PS Walker, SR Cannon SR., 1997: "*Telemetry of Forces From Proximal Femoral Replacements and Relevance to Fixation*". Journal of Biomechanics 30 225-234

Tipper, J.L., A. Hatton, J.E. Nevelos, E. Ingham, C. Doyle, R. Streicher, A.B. Nevelos, J. Fisher, 2002: "*Alumina-alumina Artificial Hip Joints. Part II: Characterization of the Wear Debris from In Vitro Hip Joint Simulations*" Biomaterials 23 3441-3448

Turell, M., A. Wang, A. Bellare "*Quantification of the Effect of the Cross-Path Motion on the Wear Rate of Ultra-high Molecular Weight Polyethylene*" Wear 255 1034-1039

Weeden, S. H., MD, W. G. Paprosky, MD, J. W. Bowling, MD, 2003: "*The Early Dislocation Rate in Primary Total Hip Arthroplasty Following the Posterior Approach with Posterior Soft Tissue Repair*". Journal of Arthroplasty 18 (6)

Walker, P.S., Ph.D., 1992: "*Design of Total Hip Replacement*" Current Orthopedics 6 (3) 146-152

Widmer, K.H., B. Zurfluh, 2004: "*Compliant Positioning of Total Hip Components for Optimal Range of Motion*" Journal of Orthopedic Research 22 815-821

APPENDIXES

Appendix A – Patient Survey Example

/

Basic Stats

Name	Phone
DOB *SEPT 3, 1922*	DOS
Sex *M*	
Occupation *RETIRED*	
Ht / Wt *5 8½ 148*	
Shoe Sizes *8½ E*	
Joint / Side *LEFT*	

Questions to ask while fluoroscoping patients

Question	Response	Comment
Did you have any previous surgery that you think effects how you perform your daily activities?	*Partial knee replacement L knee*	
Do you have any pre-existing spine, knee, ankle, hip or vascular conditions that may contribute to your hip / knee problems?	*No*	
Are you experiencing any pain, swelling, deformity or limp associated with the joint? – describe it.	*mild*	
Are you having any psychological difficulties that may effect how you perform certain activities? (stress, depression, work related accident, pending lawsuits. Etc.)	*No*	
Are there any activities that bother you in particular that involve your joint?	*No*	
How long have you had the implant?	*3 yrs 2 mos as of 12/17/03*	
Interests/ Hobbies (Physical Activities)	*Tennis*	
Reason for surgery – how did injury occur?	*Osteoarthritis*	

Things you should notice

Observation	Comment
Does the patient walk with any aids?	no
What is his / her mood?	good
Do he / she appear to be in any pain while performing the activities?	no
Do you notice any limp, swelling or any visible signs that may impede the patients ability to perform the activities?	no

Vita

Katherine Alford was born in Johnson City, TN on May 14, 1980. She attended Science Hill High School in Johnson City. She graduated from University of Knoxville, TN with an undergraduate degree in Biomedical Engineering and continued to get her masters in engineering science the following fall also at UTK. After graduating in with this masters degree she will start work at an Orthopedic Company in Memphis, TN in Knee implant design and development.